JVI Accepted Manuscript Posted Online 16 December 2020
J Virol doi:10.1128/JVI.01657-20
Copyright © 2020 Acharya et al.
This is an open-access article distributed under the terms of the Creative Commons Attribution 4.0 International license.

Accepted Manuscript Posted Online

Journal of Virology

JVI

Journal of Virology

Downloaded from http://jvi.asm.org/ on March 18, 2021 by guest

# Chronic morphine administration differentially modulates viral reservoirs in SIVmac251 infected rhesus macaque model

Arpan Acharya[a], Omalla A Olwenyi[a], Michellie Thurman[a], Kabita Pandey[a], Brenda M Morsey[b], Benjamin Lamberty[b], Natasha Ferguson[a], Shannon Callen[a], Qiu Fang[c], Shilpa J. Buch[a*], Howard S. Fox[b*], Siddappa N. Byrareddy[a*#].

## Affiliations:

[a]Department of Pharmacology and Experimental Neuroscience, University of Nebraska Medical Center, Omaha, NE, USA.

[b]Department of Neurological Sciences, University of Nebraska Medical Center, Omaha, NE, USA.

[c]Department of Biostatistics, College of Public Health, University of Nebraska Medical Center, Omaha, NE, USA.

[*]Contributed equally

[#]**Corresponding author:**

Siddappa N. Byrareddy, email: sid.byrareddy@unmc.edu

Abstract word count: 239

Text word count: 7833

**Running title:** Chronic morphine administration affects SIV reservoirs

**Key words:** Opioid Use Disorder (OUD), combined antiretroviral therapy (cART), SIV reservoirs, Tat/Rev Induced Limited Dilution Assay (TILDA), Quantitative Viral Outgrowth Assay (QVOA), Intact proviral DNA assay (IPDA).

Accepted Manuscript Posted Online

Journal of Virology

JVI

Journal of Virology

Downloaded from http://jvi.asm.org/ on March 18, 2021 by guest


## Abstract

HIV persists in cellular reservoirs despite effective combined antiretroviral therapy (cART) and there is viremia flare up upon therapy interruption. Opioids modulate the immune system and suppress antiviral gene responses, which significantly impact people living with HIV (PLWH). However, the effect of opioids on viral reservoir dynamics remain elusive. Herein, we developed a morphine dependent SIVmac251 infected *Rhesus macaque* (RM) model to study the impact of opioids on HIV reservoirs. RMs on a morphine (or saline control) regimen were infected with SIVmac251. The cART was initiated in approximately half the animals five weeks post-infection, and morphine/saline administration continued until the end of the study. Among the untreated RM, we did not find any difference in plasma/CSF or in cell-associated DNA/RNA viral load in anatomical tissues. On the other hand, within the cART suppressed macaques, there was a reduction in cell-associated DNA load, intact proviral DNA levels, and in inducible SIV reservoir in lymph nodes (LNs) of morphine administered RMs. In distinction to LNs, in the CNS, the size of latent SIV reservoirs was higher in the CD11b+ microglia/macrophages in morphine dependent RMs. These results suggest that in the proposed model, morphine plays a differential role in SIV reservoirs by reducing the CD4+ T-cell reservoir in lymphoid tissues, while increasing the microglia/ reservoir size in CNS tissue. The findings from this pre-clinical model will serve as a tool for screening therapeutic strategies to reduce/eliminate HIV reservoirs in opioid dependent PLWH.

Accepted Manuscript Posted Online

Journal of Virology

JVI

Journal of Virology

Downloaded from http://jvi.asm.org/ on March 18, 2021 by guest

## Importance

Identification and clearance of HIV reservoirs is a major challenge in achieving a cure for HIV. This is further complicated by co-morbidities that may alter the size of the reservoirs. There is an overlap between the risk factors for HIV and opioid abuse. Opiates have been recognized as prominent co-morbidities in HIV-infected populations. People infected with HIV also abusing opioids have immune modulatory effects and more severe neurological disease. However, the impact of opioid abuse on HIV reservoirs remains unclear. In this study, we used morphine dependent SIVmac251 infected rhesus macaque (RM) model to study the impact of opioids on HIV reservoirs. Our studies suggested that people with HIV who abuse opioids had higher reservoirs in CNS than the lymphoid system. Extrapolating the macaque findings in humans suggests that such differential modulation of HIV reservoirs among people living with HIV abusing opioids could be considered for future HIV cure research efforts.

Accepted Manuscript Posted Online

Journal of Virology

JVI

Journal of Virology

Downloaded from http://jvi.asm.org/ on March 18, 2021 by guest

## Introduction

Opioid use disorder (OUD) is a chronic illness characterized by persistent use of opioids to the detriment of the user (1). Globally, there was an estimated 26.8 million people living with OUD in 2016(1), of which 2.1 million were from USA (2). People living with OUD are at higher risk of medical comorbidities including human immunodeficiency virus (HIV) and Hepatitis C (HCV) infection (3). Worldwide, it is estimated that 80% of injection drug users take opioids and 17.8% of them are HIV positive (4, 5). Epidemiological studies have shown that chronic opioid administration is immunosuppressive, downregulates the antiviral genes, and increases the susceptibility to infections like tuberculosis and HIV (6-12). The innate and adaptive immune responses act in synchrony against the invading pathogens, and opioids acting through the opioid receptors alter both these responses (13, 14).

OUD is important in the context of HIV infection, as several studies have reported that PLWH who use opioids are at a higher risk of developing neurological disorders compared to PLWH without OUD (15-20). Opioids have been shown to upregulate the expression of CCR5 while downregulating the expression of its cognate β-chemokine production by acting through μ-opioid receptor in macrophages and microglia, thereby boosting the entry of R5 tropic viruses in these target cells (21-24). Opioids and HIV synergistically act to activate glia and upregulate the expression of cytokines and chemokines, leading, in turn, to neuronal damage and development of hyperalgesia (25-27).

One barrier to the cure of HIV is that the HIV genome integrates into the host chromosome (28). A subset of infected cells with integrated proviral DNA can enter a

Accepted Manuscript Posted Online

Journal of Virology

JVI

Journal of Virology

Downloaded from http://jvi.asm.org/ on March 18, 2021 by guest

92 transcriptionally silent state that can persist in the context of combination antiretroviral
93 therapy (cART) and escape host cell immune surveillance owing to its inability to
94 produce antigens essential for triggering immune responses. This, in turn leads to
95 creation of a pool of long-lived viral reservoirs (29). HIV reservoirs are seeded early
96 after infection and persist through the entire lifetime of the host. Among all the cellular
97 reservoirs, resting memory CD4+ T cells are the best characterized, though persistence
98 of viral reservoirs in perivascular macrophages and microglia in central nervous system
99 (CNS) has also been reported (30, 31). Active and latent reservoirs of HIV also persist
100 in several other tissues owing to the presence of subtherapeutic concentrations of
101 antiretrovirals in these tissue locations. The major barriers to penetration of ART in deep
102 tissues are their physiochemical properties and the presence of drug efflux transporters
103 (32) among the well-characterized tissue reservoirs such as LNs, spleen, gut associated
104 lymphoid tissues (GALT) and the thymus (33). The other less characterized anatomical
105 tissue reservoirs of HIV include the kidney, liver, lung, bone marrow, genital tract and
106 CNS (34-36).
107 Morphine and other frequently used/abused opioids have been shown to inhibit the
108 phagocytic property of macrophages, migration of neutrophils, and have a cytopathic
109 effect on NK cells, which in combination results in dampening of the innate immune
110 system (37). During adaptive immune responses, chronic morphine exposure leads to
111 defective antigen presentation and a phenotype switch from Th1 to Th2 in CD4+ T cells
112 resulting in inhibition of pro-inflammatory responses that are critical for eradicating
113 invading intracellular pathogens (38). Interestingly, there are also conflicting reports
114 refuting the immune suppressive effects of morphine, with some reports from rodent

Accepted Manuscript Posted Online

Journal of Virology

JVI

Journal of Virology

Downloaded from http://jvi.asm.org/ on March 18, 2021 by guest

models and studies using ex vivo human samples indicating activation of the pattern recognition receptor TLR4 and subsequent cellular activation (39-43).

There are multiple lines of evidence implicating the role of morphine in mediating immunosuppressive effects in the periphery, its role in infectivity, transmission, and pathogenesis of HIV and its potentiation of HIV neuropathogenesis (16, 21, 24, 44, 45). However, the role of morphine in modulating the persistence of HIV reservoirs in various anatomical sanctuaries remains elusive. In the present study, we sought to examine the impact of morphine dependency on the size of simian immunodeficiency virus (SIV) reservoirs using the SIVmac251-infected rhesus macaque (RM) model. SIV reservoirs were found to persist in all the major cellular and tissue locations in ART-suppressed, morphine-dependent, and saline administered rhesus macaques. Our findings suggest that morphine differentially modulates the size of viral reservoirs in lymphoid tissues versus the CNS. To the best of our knowledge, this is the first study to report differential regulation of viral reservoir dynamics in the context of opioid dependence and warrants further investigation to dissect the molecular mechanism(s).

## Results

**Dynamics of plasma and cerebrospinal fluid (CSF) viral loads in morphine dependent versus control SIVmac251 infected rhesus macaques with and without antiretroviral therapy.**

In this study, we included a total 19 macaques. Ten (n=10) RM were ramped up over two weeks to a final dosage of 6 mg/kg morphine administered twice daily, which was

Accepted Manuscript Posted Online

Journal of Virology

JVI

Journal of Virology

Downloaded from http://jvi.asm.org/ on March 18, 2021 by guest

maintained for seven weeks, while nine (n=9) RMs received saline and served as the control. At week 9, all the macaques were inoculated with a single 200 $TCID_{50}$ dose of SIVmac251 by intravenous injection. Five weeks post-inoculation cART was initiated in six out of ten RMs in the morphine group and in five out of nine RMs in the control group. Four monkeys from each group were left untreated until the end of the study (Fig 1). Within the control group (n=9), the median peak plasma viral load was $1.25X10^7$ SIV copies/ml and median peak CSF viral load was $1.02X10^5$ SIV copies/ml respectively. On the other hand, in the morphine administered group (n=10), the median peak plasma and CSF viral load was 8.68 $X10^7$ SIV copies/ml and $4.62X10^4$ SIV copies/ml (Fig 2 A, B, E, F). All eleven animals from the antiretroviral treated group became aviremic with completely suppressed plasma and CSF viral load within 13 weeks post-inoculation, which is equivalent to 8 weeks of antiretroviral therapy, and they remained virally suppressed until the end of this study (Fig 2 E, F). The longitudinal geometric mean of plasma and CSF viral loads between morphine vs. saline treated RMs in all the groups is presented in Fig 2 C, D, G, H.

**Cell-associated SIV DNA/RNA in the blood, lymph nodes and rectal mucosal tissues.**

To understand how chronic morphine administration could modulate the size of SIV reservoirs in various tissue compartments in the presence and/or absence of cART, we sought to quantify the cell-associated SIV DNA and RNA in various anatomical tissue sanctuaries collected during necropsy of all the RMs included in this study. Since CD4+ T cells are known to be the major contributor to viral reservoirs in both the blood and LNs, CD4+ T cells were purified from peripheral blood and LNs followed by isolation of

Accepted Manuscript Posted Online

Journal of Virology

JVI

Journal of Virology

Downloaded from http://jvi.asm.org/ on March 18, 2021 by guest

161 DNA/RNA as described in Material and Methods. In PBMCs of ART naïve RMs, the
162 median cell-associated SIV DNA load was 15,898 copies/$10^6$ CD4+ T cells in morphine
163 administered group versus 8,547 copies/$10^6$ CD4+ T cells in saline controls (p=0.600).
164 In the PBMCs of ART treated RMs, the median cell-associated SIV DNA load was 3,332
165 copies/$10^6$ CD4+ T cells in morphine administered group versus 4,583 copies/$10^6$ CD4+
166 T cells in saline controls (p=0.055) (Fig 3A). Similarly, in PBMCs of ART naïve RMs, the
167 median cell-associated SIV RNA load was 30,533 copies/$10^6$ CD4+ T cells in morphine
168 administered group versus 18,890 copies/$10^6$ CD4+ T cells in saline controls (p=0.990).
169 In the PBMCs of the ART treated group, the median cell-associated SIV RNA load was
170 94 copies/$10^6$ CD4+ T cells in morphine administered group versus 446 copies/$10^6$
171 CD4+ T cells in controls (p=0.120) (Fig 3B).

172 Next, we measured the cell-associated DNA and RNA in CD4+ T cells purified from
173 LNs. In LNs of ART naïve RMs, the median cell-associated SIV DNA load was 11,295
174 copies/$10^6$ CD4+ T cells in morphine administered group versus 14,962 copies/$10^6$
175 CD4+ T cells in saline controls (p=0.600). On the other hand, in LNs of the ART group a
176 significant difference was found, with a median cell-associated SIV DNA load of 4,392
177 copies/$10^6$ CD4+ T cells in morphine administered group versus 7,847 copies/$10^6$ CD4+
178 T cells in saline controls (p=0.008) (Fig 3C). In LNs of ART naïve RM, median cell-
179 associated SIV RNA was 330,802 copies/$10^6$ CD4+ T cells in morphine administered
180 group versus 968,610 copies/$10^6$ CD4+ T cells in saline controls (p=0.220). In the LNs
181 of ART treated group, median cell-associated SIV RNA load was 143 copies/$10^6$ CD4+
182 T cells in morphine administered group versus 260 copies/$10^6$ CD4+ T cells in saline
183 controls (p=0.360) (Fig 3D).

Accepted Manuscript Posted Online

Journal of Virology

JVI

Journal of Virology

Downloaded from http://jvi.asm.org/ on March 18, 2021 by guest

Further, we assessed cell-associated DNA and RNA in mucosal tissue collected from the rectum during necropsy. In the ART naïve RMs median cell-associated SIV DNA load was 1,201 copies/$10^6$ cells in morphine administered group versus 10,961 copies/$10^6$ cells in saline controls (p=0.342). In the ART treated group, a significant difference was found, with a median cell-associated SIV DNA load of 70 copies/$10^6$ cells in morphine administered group versus 272 copies/$10^6$ cells in saline controls (p=0.036) (Fig 3E). In ART naïve RMs, median cell-associated SIV RNA load was 368,990 copies/$10^6$ cells in morphine administered group versus 341,883 copies/$10^6$ cells in saline controls (p=0.885). In the ART treated group, the median cell-associated SIV RNA load was 11 copies/$10^6$ cells in morphine administered group versus 39 copies/$10^6$ cells in saline controls (p=0.080) (Fig 3F).

We also measured the cell-associated DNA/RNA in both the spleen and lungs of macaques. There was no difference in cell-associated SIV DNA/RNA level in the lungs nor spleen of the morphine administered versus saline controls in the presence of ART treatment as well as the ART naïve RMs (Fig 4). In summary, we found significant reduction in cell associated DNA viral loads within LNs and rectal mucosal tissue in morphine administered cART treated animals when compared with saline controls.

**Quantitation of SIV reservoirs in CD4+ T cells of blood and lymph nodes.**

We used the Tat/rev Induced Limiting Dilution Assay (TILDA) to measure the size of inducible SIV reservoirs in the blood and LNs of morphine/saline administered, SIV-infected, cART-treated RMs (Fig 1). In peripheral blood, the median frequency of CD4+ T cells producing inducible multiply splices (ms)-Tat/rev transcript per million of CD4+ T

Accepted Manuscript Posted Online

Journal of Virology

JVI

Journal of Virology

Downloaded from http://jvi.asm.org/ on March 18, 2021 by guest

206 cells was 4.54 in morphine administered group versus 9.11 in the saline control group
207 (p=0.067) (Fig 5A). In the LNs, the median frequency of CD4+ T cells producing
208 inducible ms-Tat/rev transcript per million of CD4+ T cells was 6.47 in morphine
209 administered group versus 10.38 in the saline control group which was statistically
210 significant (p=0.036) (Fig 5B).

211 We next used the intact proviral DNA assay (IPDA) to estimate the size of replication
212 competent SIV reservoirs in both the blood and LNs. Recently Bruner et al., developed
213 a multiplex droplet digital PCR (ddPCR) based HIV-1 proviral DNA quantification assay
214 that can distinguish between intact versus defective proviruses and is referred to as
215 IPDA. The authors have described a positive correlation and identical decay rate of viral
216 reservoirs when measured by quantitative viral outgrowth assay (QVOA) and IPDA (46).
217 Bender et al., have reported adaptation of IPDA for quantification of the intact SIV
218 genome in ART suppressed rhesus macaques, implicating thereby its utility to serve as
219 a surrogate marker to measure size of latent reservoirs (47). Herein, using IPDA, we
220 measured the frequency of intact SIV genome in both blood and LNs of morphine/saline
221 administered as well as SIV-infected cART treated RM (Fig 1). In CD4+ T cells purified
222 from peripheral blood, the median of intact SIV genome per million cells was 1,480 for
223 the morphine administered group versus 2,521 in the saline control group (p=0.080) (Fig
224 5C). However, in the CD4+ T cells purified from LNs, the median of intact SIV genome
225 per million cells, measured at 2,789 for the morphine administered group versus 4,399
226 in saline control group (p=0.036) (Fig 5D).

227

Accepted Manuscript Posted Online

Journal of Virology

JVI

Journal of Virology

Downloaded from http://jvi.asm.org/ on March 18, 2021 by guest

**Changes in CD4+ T cell polarization in PBMCs and Lymph nodes**

Chronic morphine exposure depletes lymphoid cells and leads to a phenotypic switch of Th1 to Th2 in CD4+ T cells (38). On the other hand, a recent report suggests that in chronic HIV patients, the majority of intact replication competent proviruses persists in Th1 polarized CD4+ T cells (48). To understand the impact of chronic morphine administration on T lymphocytes, flow cytometry was performed at necropsy to determine the CD4+ T cell polarity in the PBMCs and LNs of cART treated RMs. In PBMC, to differentiate between Th1, Th2, and Th17 cells, intracellular cytokine staining was performed as described earlier (49). Due to poor cytokine production by LN germinal center Tfh cells, it is difficult to differentiate Tfh subpopulations by cytokine production assays (50). Therefore, we performed surface staining of chemokine receptors of Tfh cells (CD95+PD1+CXCR5+) from LNs to identify Th1 like Tfh (CXCR3+), Th2 like Tfh (CCR4+), and Th17 like Tfh (CCR6+) subpopulations (51). The gating strategies used for PBMCs and LNs is described in Fig 6, 7, and 8. In PBMCs, the frequency of CD4+ Th1 polarized cells was measured by quantifying levels of IFNγ and TNFα cytokine secreting cells. In morphine administered RMs, IFNγ secreting cells had a median of 0.87% versus 1.55% (p=0.536) for controls (Fig 9A), while TNFα secreting cells had median of 5.61% versus 14.70% for controls, which was significantly different (p=0.017) (Fig 9B). The median of IL-4 secreting Th2 polarized CD4+ T cells in the morphine administered macaques was 2.55% versus 1.76% in saline controls (p=0.305) (Fig 9C). The levels IL-17 secreting CD4+ Th17 lymphocytes in the morphine treated group had a median of 0.47% versus 0.48% in saline controls (p=0.930) (Fig 9D). Remarkably, exposure to morphine in cART-treated SIV-infected

Accepted Manuscript Posted Online

Journal of Virology

JVI

Journal of Virology

Downloaded from http://jvi.asm.org/ on March 18, 2021 by guest

251 RMs led to a significant elevation of CD4+ Treg lymphocytes with a median of 5.22%
252 versus 2.95% in the saline control group (p=0.004) (Fig 9E).

253 Within the LNs, morphine administered cART treated RMs had lower frequencies of T
254 follicular helper cells (Tfh) expressing PD-1, CXCR5 and CD95 with a median value of
255 7.61% versus 13.49% in saline control groups (p=0.017) (Fig 9F). On the other hand, in
256 the morphine administered group the frequency of regulatory Tfh (CD25+FoxP3+ Tfh)
257 cells was elevated with a median of 8.78% versus 2.87% in saline control group
258 (p=0.030) (Fig 9G). Similarly, there was an elevation of CD4+CXCR5- Treg
259 (CD25+FoxP3+) cells in morphine administered group with a median of 4.57% versus
260 1.25% in saline control group (p=0.004) (Fig 9H). Evaluation of Tfh cell polarity was also
261 carried out as shown by the representative sample in Fig 9I. There were differences in
262 Tfh cell differentiation (Th1 vs Th2) in morphine administered group versus saline
263 controls. In the morphine group, while there was a reduction in CXCR3+Tfh cells (Th1)
264 with a median of 47.70% versus 56.30% in saline control group (p=0.004) (Fig 9J), there
265 was an elevation in CCR4+Tfh cells (Th2) with a median of 18.70% in the morphine
266 administered group versus 8.49% in the saline control group (p=0.004) (Fig 9K).
267 Further, CCR6+Tfh cells (Th17) had a median of 55.95% in the morphine administered
268 RMs versus 60.40% in saline control RMs (p=0.792) (Fig 9L). Finally, differences in
269 immune activation across different cell subsets were evaluated. Fig 9M denotes
270 representative sample for CD4+ T cell activation. For CD4+ T cell activation (denoted by
271 CD4+/CD38+/ HLA-DR+), the morphine administered RMs had a significantly lower
272 frequency with a median of 3.37% versus 6.13% in saline controls (p=0.017) (Fig 9N).
273 Similarly, for B cell activation (denoted by CD20+/CD38+/HLA-DR+), the morphine

Accepted Manuscript Posted Online

Journal of Virology

JVI

Journal of Virology

Downloaded from http://jvi.asm.org/ on March 18, 2021 by guest

administered macaques had a significantly reduced frequency with a median of 27.10% versus 53.50% in saline controls (p=0.017) (Fig 9O). On the other hand, for NK cell activation (CD3-/CD8α/CD38+/HLA-DR+), the morphine administered group had a median frequency of 11.45% versus 9.16% in the saline control group (p=0.428) (Fig 9P).

**Quantification of SIV reservoirs in the CNS.**

To understand how chronic morphine administration impacted the seeding and persistence of viral reservoirs in the CNS, we analyzed CD11b+ myeloid cells (microglia and perivascular macrophages) from the brains of the cART-treated morphine administered and saline control SIV-infected monkeys, all of which had complete viral suppression in the plasma and CSF (below 50 copies/ml). Immediately after necropsy CD11b+ cells were purified from brains. After purification, we obtained more than 95% cells positive for CD11b (Fig 10)**.** The median of cell associated DNA load was 50.5 copies per million CD11b+ microglia/macrophages in the morphine administered group versus 0 in the saline control group (p=0.350) (Fig 11A). The median cell-associated RNA load was 32.5 copies per million CD11b+ microglia/macrophages in morphine administered group versus 15 in the saline control group (p=0.710) (Fig 11B)**.** We next sought to estimate the size of latent replication-competent SIV reservoirs in CD11b+ microglia/macrophages using macrophage QVOA (MØ-QVOA). The number of CD11b+ macrophages used for the MØ-QVOA for each animal is described in Table 1. On average, we detected 0.075% CD3+ T cells within the enriched CD11b+ cells from brain, which is in line with 0.06% reported by Avalos et al., (52). Based on percentage of CD4+ T cells out of total CD3+ T cells, and the frequency of CD4+ T cells having intact

Accepted Manuscript Posted Online

Journal of Virology

JVI

Journal of Virology

Downloaded from http://jvi.asm.org/ on March 18, 2021 by guest

proviral genome (as determined by IPDA), the probability of the presence of CD4+ T cells with intact proviral genome in any sample of macrophage quantitative outgrowth assay was found to be less than one. The CD11b+ microglia/macrophages obtained from morphine administered macaques had a median infectious unit per million (IUPM) value of 0.89 versus 0.19 in saline control group (p=0.014) (Fig 11C), indicating presence of a significantly higher number of cells carrying infectious SIV in the morphine group.

## Discussion

In order to achieve a functional cure of HIV-1, the primary goal is to identify all cell types and anatomical sanctuaries of viral reservoirs and to understand the molecular mechanism of their long-term persistence. Substantial work has already been done to characterize and understand the underlying mechanism of latent reservoirs in circulating CD4+ T cells and in lymphoid tissues. Several lines of evidence suggest that HIV enters the CNS within 3-7 days of infection as well as tissue resident macrophages and microglia, which likely serve as viral reservoirs and are a source of viral rebound in case of therapeutic interruptions (34, 53-55). The mechanism of persistence of HIV reservoirs in myeloid cells is still unknown (35). Substance use disorders (SUD) and more specifically OUD, are an important co-morbidity among PLWH (23). Opioids have immune modulatory effects and mostly render macrophages more permissive to HIV infection (21, 24, 56, 57). However, the impact of opioids on seeding and persistence of HIV reservoirs remains underscored and this gap poses a major roadblock in HIV cure research. To shed some light on this direction, in the present study we used SIVmac251

Accepted Manuscript Posted Online

Journal of Virology

JVI

Journal of Virology

Downloaded from http://jvi.asm.org/ on March 18, 2021 by guest

320 infected rhesus macaques as a non-human primate (NHP) model of HIV infection to
321 understand how opioid use could modulate the size of viral reservoirs. We chose the
322 SIVmac251 stock for intravenous infection since it contains multiple quasispecies of
323 varying tropism (58), and IVDU are often initially infected by multiple transmitted viral
324 sequences (59). Recently Abreu et al. showed that indeed ART-suppressed SIVmac251
325 rhesus macaques are an ideal model for studying the viral reservoirs from different
326 anatomical tissue sanctuaries (60).
327 The results of the present study indicate there was no difference in geometric mean of
328 plasma and CSF viral loads between morphine administered versus control animals
329 receiving saline in both untreated and ART suppressed groups. However, in a previous
330 study, Bokhari et al., reported that morphine administered rhesus macaques exhibited
331 one log higher plasma and CSF viral load compared to controls. It should be noted that
332 there are a couple of differences between the study of Bokhari et al., and the current
333 study. Bokhari et al., administered morphine in four equal doses daily, whereas we
334 administered two equal daily doses. Since the plasma half-life of morphine is around
335 two and half hours (61), the difference in dosage could lead to variances in the mean
336 effective plasma concentration of the drug. Further, while we used SIVmac251, Bokhari
337 et al., used a brain-derived stock of SIV (SIVmacR71/17E) (18). In the Bokhari et al.,
338 study a high rate of rapid progression of disease was found in the morphine treated
339 group, and similar findings were obtained by Kumar et al., using a mixture of different
340 SIVs (SHIV(KU), SHIV(89.6)P, and SIV/17E-Fr) (62). Furthermore, as the rhesus
341 macaques used in different studies are outbred from multiple colonies, it is expected
342 that there would be a wide variation in their genetic background, and subsequently their

Accepted Manuscript Posted Online

Journal of Virology

JVI

Journal of Virology

Downloaded from http://jvi.asm.org/ on March 18, 2021 by guest

343 response to morphine administration and SIV disease pathogenesis. These differences
344 could have contributed to the differences of plasma and CSF viral loads observed in
345 these studies.
346 Among the untreated RMs, we did not find any difference in cell-associated DNA and
347 RNA loads at different tissue compartments between morphine administered and the
348 saline control group. On the other hand, in cART suppressed RMs, we observed a
349 significant reduction in cell-associated DNA load in CD4+ T cells obtained from LNs as
350 well as in tissue samples collected from rectal mucosa in morphine administered
351 macaques compared to saline controls. This finding is substantiated by IPDA and
352 TILDA performed on CD4+ T cells purified from LNs, where the number of intact SIV
353 genome per million CD4+ T cells is less and the size of inducible SIV reservoirs in
354 CD4+ T cells is lowered significantly in morphine administered RMs compared to saline
355 controls respectively. These findings indicate that chronic morphine administration in
356 combination with ART have a positive impact on lowering SIV reservoirs in lymphoid
357 tissues.
358 The CD4+ T cells are a major source of latent reservoirs of HIV in lymphoid tissues like
359 LNs, GALT, and in peripheral blood among others (63). In LNs HIV reservoirs seeded
360 during acute infection, associated with virus production and storage of viral particles in
361 immune complexes, and Tfh cells constitute the major part of LN viral reservoirs (64-
362 66). We observed depletions of Tfh cells in LNs of morphine administered macaques
363 that supports earlier reports that chronic morphine abuse depletes the volume and total
364 number of lymphoid cells from LNs (67, 68). Brown et al., reported that morphine
365 induces an immune-suppressive effect in LNs and peripheral blood of African green

Accepted Manuscript Posted Online

Journal of Virology

JVI

Journal of Virology

Downloaded from http://jvi.asm.org/ on March 18, 2021 by guest

366 monkeys and pigtailed macaques with a substantial decrease in abundance of several
367 metabolic proteins involved in energy metabolism pathways accompanied by significant
368 decreases in activated $CD4^+$/ $CD8^+$ T cells (69). Therefore, we speculate, in our
369 experimental setting that chronic morphine administration may dampen the T-cell
370 activation and suppress their metabolic activity and cause a reduction in seeding of SIV
371 in CD4+ T cells during acute stage of infection before initiation of cART, which may
372 result in smaller size of persistent latent SIV reservoirs in CD4+ T cells of morphine
373 administered animals compared to control macaques that received saline.
374 Next, we observed that morphine administration resulted in the expansion of regulatory
375 T cells in peripheral blood as well as in LNs, that have been previously reported to
376 suppress T-cell activation (70). In LNs, we also observed lower level of activation of
377 CD4+ T cells and B cells in morphine administered animals compared to saline controls.
378 This supports the proposed mechanism of morphine mediated reduction on SIV
379 reservoirs within the lymphoid tissue compartments. In the LNs of morphine
380 administered animals we observed a reduction in frequency of CXCR3+Th1 like Tfh
381 cells and expansion of CCR4+Th2 like Tfh cells and it was reported earlier that Th1 like
382 Tfh cells enter LN germinal center during acute stage of HIV/SIV infection, express high
383 level of CCR5, and constitute a major part of viral reservoirs in LNs (71-73). In
384 combination, findings above may lead to depletion of functional SIV reservoirs in CD4+
385 T cells of morphine administered ART suppressed rhesus macaques (Fig 12A).
386 Contrary to the CD4+ T cells, we observed an opposite effect of morphine in modulation
387 of the viral reservoir in CNS. The median size of replication competent SIV reservoirs in
388 CD11b+ microglia/macrophages from the brain is significantly higher in morphine

Accepted Manuscript Posted Online

Journal of Virology

JVI

Journal of Virology

Downloaded from http://jvi.asm.org/ on March 18, 2021 by guest

389 administered RMs compared to control animals receiving saline. There are several
390 factors that may be responsible for the morphine-mediated modulation of CNS SIV
391 reservoirs. It has been reported that morphine upregulates the expression of CCR5
392 coreceptor in macrophages, which, in turn, could increase the viral permissiveness of
393 these cells (21, 57, 74). Morphine is known to also lower the CNS penetration of several
394 antiretrovirals which could result in ongoing viral replication in the CNS and be
395 responsible for the larger reservoir (75). Again, it has been shown that morphine alone
396 or in combination with HIV TAT increases the permeability of blood brain barrier (BBB)
397 and increases trans-endothelial migration of leucocytes by activation of proinflammatory
398 cytokines, intracellular $Ca_2$+ release, and activation of myosin light chain kinase that
399 downregulate tight junction proteins and decrease transendothelial electric resistance
400 (26, 76, 77). It also increases the release of CCL2, CCL5, and IL-6 by astrocytes and
401 upregulates expression of ICAM and VCAM on brain vascular endothelial cells that
402 promote trafficking of HIV infected peripheral leucocytes in CNS (78). Morphine is also
403 shown to downregulate the expression of anti-HIV microRNAs and impair the function of
404 anti-HIV restriction factors in monocytes (79, 80). Taken together, these could lead to
405 increased size of the viral reservoirs in the CNS of morphine administered group in
406 comparison to the controls that received saline (Fig 12B). We observed a similar
407 analogy with our finding of differential modulation of SIV reservoirs by morphine in T
408 cells from PBMC/LNs versus microglia/macrophages in CNS in some previous reports
409 where phenelzine, a monoamine oxidase (MAO) inhibitor, suppressed reactivation of
410 HIV in T cells (81) and reactivated HIV in human microglia cell lines (82). To the best of

Accepted Manuscript Posted Online

Journal of Virology

JVI

Journal of Virology

Downloaded from http://jvi.asm.org/ on March 18, 2021 by guest

our knowledge this is the first report of opioid mediated differential modulation of HIV reservoirs using macaque models of HIV infection.

The major caveat of the current study is the number of RMs included in each group due to the prohibitive cost of conducting long-term studies with multiple daily injections. Other issues include the experimental design where animals were initially ramped-up with morphine, then infected, and then treated with cART. In a patient cohort, this may not be an ideal scenario, as most of the people suffering from substance use disorders take multiple forms of drugs. Furthermore, opioid use may follow infection, for example in PLWH, opioids are prescribed to treat chronic pain, and subsequently they may become addicted to these substances. For this population, how opioids use modulates the dynamics of different viral reservoirs needs to be explored. In addition, given the different cellular nature of the reservoir (CD4+ T cells in lymphoid tissues and macrophages in the CNS) the possible effects of opioids on viral tropism is unknown.

In conclusion, for the first time we describe a morphine dependent SIVmac251 infected RM model to study the impact of opioid use disorder (OUD) on HIV reservoirs. Our results suggest that morphine differentially modulates SIV reservoirs in LNs and rectal mucosal tissue versus SIV reservoirs in myeloid lineage of cells within the CNS. Chronic morphine administration reduces the size of viral reservoirs in CD4+ T cells in LNs, and increases the size of SIV reservoirs in brain resident CD11b+ macrophages. We propose that these pre-clinical models will serve as a tool to discover the molecular mechanism of opioid mediated differential regulation of viral reservoirs among PLWH and suffering from OUD.

Accepted Manuscript Posted Online

Journal of Virology

JVI

Journal of Virology

Downloaded from http://jvi.asm.org/ on March 18, 2021 by guest

434 ## Materials and Methods

435 ### Reagents and cell lines

436 Antiretroviral drugs tenofovir alafenamide (TFV) and emtricitabine (FTC) were
437 obtained from Gilead Sciences, Foster City, CA, USA, while dolutegravir (DTG) was
438 procured from ViiV Healthcare, Research Triangle Park, NC, USA as MTA with Dr.
439 Byrareddy. All other molecular biology grad fine chemicals used in the study were
440 purchased from Sigma-Aldrich, St. Louis, MO, USA unless otherwise mentioned.
441 CEMx174 is a hybrid human lymphoid cell line generated from human B721.174 and
442 T-CEM cell lines, that was used for expansion of virus in quantitative viral outgrowth
443 assays due to its enhanced susceptibility to SIV infection(83). This cell line was
444 provided by Dr. J. Hoxie (University of Pennsylvania, Philadelphia). CEMx-174 cells
445 were maintained in complete RPMI (RPMI-1640 (Gibco; Cat# 21870076), 10% heat-
446 inactivated fetal bovine serum (FBS) (Gibco; Cat#10437-028), 2 mM L-Glutamine
447 (Gibco; Cat#35050079) and 100 U/ml penicillin and 100 ug/ml streptomycin (Gibco;
448 Cat#15140-122)) at 37°C and 5% $CO_2$.

449 ### Animals and Ethical statement

450 A total of nineteen Indian origin, outbred, pathogen free RMs (*Macaca mulatta*, mean
451 age: 4.67 years range: 4.1 to 7.0 years) were used in this study (Table 2). Macaques
452 were housed in compliance with the regulations under the Animal Welfare Act, the
453 Guide for the Care and Use of Laboratory Animals in the nonhuman primate facilities at

Accepted Manuscript Posted Online

Journal of Virology

JVI

Journal of Virology

Downloaded from http://jvi.asm.org/ on March 18, 2021 by guest

454 the Department of Comparative Medicine, University of Nebraska Medical Center
455 (UNMC), Omaha, Nebraska, USA. Animals were maintained in a temperature controlled
456 (72ºF) indoor climate with 12-hour light/dark cycle. The monkeys were observed twice
457 daily for development of distress or disease by the animal care staffs and veterinary
458 personnel. The animals were daily fed monkey diet (Purina) supplemented with fresh
459 fruit or vegetables and water ad libitum.

460 At the end of the study, all RMs were humanely euthanized using a high dose of
461 ketamine/zylazine and then the thoracic cavity was opened and perfused/exsanguinated
462 according to the guidelines of the American Veterinary Medical Association. This study
463 was reviewed and approved by UNMC Institutional Animal Care and Use Committee
464 (IACUC) and the Institutional biosafety Committee (IBC) under protocol number '16-
465 073-07-FC' titled "The effect of cART and drug of abuse on the establishment of CNS
466 viral reservoirs" and '15-113-01-FC' titled "The combinatorial effects of Opiates and
467 promoter-variant strains of HIV-1 subtype C on neuropathogenesis and latency". UNMC
468 has been accredited by the Association for Assessment and Accreditation of Laboratory
469 Animal Care International.

470 **Study Design**

471 The overall design of the study is illustrated in a schematic form in Fig 1. These
472 experiments were designed to investigate the effect of chronic morphine administration
473 on the establishment of viral reservoir in SIV-infected RMs in different anatomical
474 compartments of the body. The study included 19 juvenile RMs. The RMs were

Accepted Manuscript Posted Online

Journal of Virology

JVI

Journal of Virology

Downloaded from http://jvi.asm.org/ on March 18, 2021 by guest

475 randomly divided into two groups. One group had ten animals which were ramped-up
476 over two weeks to a final 6 mg/kg intramuscular injection of morphine administered
477 twice daily, which was then maintained for seven weeks and the other group (n=9)
478 received a similar dose of normal saline (control group). At this point all the macaques
479 were intravenously inoculated with 200 $TCID_{50}$ of SIVmac251 (viral stock was obtained
480 from Dr. Mahesh Mohan from Tulane National Primate Research Center), while the
481 administration of morphine/saline continued until the end of the study. After five weeks
482 post-inoculation, daily ART was initiated in six macaques from morphine group and five
483 macaques in the control group and continued until the end of the study. ART regimen
484 consisted of two reverse transcriptase inhibitors (FTC: 40 mg/ml and TFV: 20 mg/ml)
485 and one integrase inhibitor (DTG: 2.5 mg/ml). All the drugs were dissolved in a vehicle
486 made up of 15% Kleptose HPB (Roquette, parenteral grade) (w/w) in 0.1N NaOH. The
487 anti-retroviral drugs were administered subcutaneously once daily at 1 ml/kg body
488 weight. Peripheral blood from the femoral vein, CSF by direct puncture of the cisterna
489 magna or by lumbar puncture, LNs and colorectal mucosa biopsies were collected
490 longitudinally at different time points of the study after anesthetizing the monkeys with
491 ketamine-HCl (5-20 mg/kg) or telazol (3-5 mg/kg) to monitor SIV viral loads and a series
492 of immunologic and virologic parameters as described in experimental schema.

493 **SIV plasma and CSF viral load quantification**

494 SIV RNA concentration in the plasma and CSF samples were measured by quantitative
495 reverse transcription-PCR (qRT-PCR) as previously described(84). In brief, plasma was
496 separated from blood samples collected in K2-EDTA vacutainer tubes (Becton

Accepted Manuscript Posted Online

Journal of Virology

JVI

Journal of Virology

Downloaded from http://jvi.asm.org/ on March 18, 2021 by guest

497 Dickinson, San Diego, California, USA) within 4 hours of collection. RNA was extracted
498 from 140 µl of plasma and CSF samples using a QIAamp Viral RNA mini kit according
499 to manufacturer's instructions (QIAGEN Germantown, MD, USA; Cat# 52906). SIV gag
500 RNA was quantified by qRT-PCR using the TaqMan RNA-to-Ct 1-Step Kit (Thermo
501 Fisher Scientific, MA; Cat# 4392938) and Applied Biosystems QuantStudio 3 Real-Time
502 PCR System (Applied Biosystems, Waltham, MA, USA). Primers and probes used for
503 SIV gag RNA quantification were as follows: SIVGAGF: 5' –
504 GTCTGCGTCATCTGGTGCATTC – 3'; SIVGAGR: 5' –
505 CACTAGGTGTCTCTGCACTATCTGTTTTG – 3' and SIVP: 5'- /6-FAM/ CTTCCTCAG
506 /ZEN/ TGTGTTTCACTTTCTCTTCTGCG /3IABkFQ/ - 3'.

507 **Purification of CD4+ T cells:**

508 Peripheral blood mononuclear cells (PBMCs) and LN cells were enriched for CD4+ T
509 cells using the EasySep NHP CD4+ T cell isolation kit from STEMCELL Technologies
510 Canada Inc (Cat#: 19582) as per the manufacturer's instruction. Briefly, frozen cells
511 were thawed at 37°C, washed with complete RPMI (composition described above),
512 centrifuged for 6 min at 1200rpm, and resuspended in 1 ml of recommended medium
513 (Phosphate Buffered Saline (PBS) containing 2% Fetal Bovine Serum (FBS) and 1 mM
514 EDTA). The cell suspension was transferred to a 12x75 mm polystyrene tube, 50 µl of
515 EasySep Negative Selection cocktail was added, mixed well and the cell suspension
516 was incubated at room temperature (RT) for 10 minutes. Then 100 µl of EasySep
517 Magnetic Particles were added and the cells were incubated at RT for 5 minutes. After
518 incubation, 2 ml of recommended medium was added to the solution, then the tubes

Accepted Manuscript Posted Online

Journal of Virology

JVI

Journal of Virology

Downloaded from http://jvi.asm.org/ on March 18, 2021 by guest

were placed in an EasySep magnet for 5 min. The negatively selected enriched CD4+ T cells were collected for downstream applications.

**Isolation of total myeloid-enriched brain cells:**

Myeloid-enriched brain isolation used a modification of the procedure described by Marcondes et al., (85). In brief, the brain was sectioned and meninges removed in Hank's balanced salt solution (HBSS; Invitrogen, Carlsbad, CA). The cleaned-tissue was homogenized with a dounce homogenizer and washed twice with HBSS. Brain homogenate was digested on a rotating platform at 37° C for 30 minutes in HBSS with 28 U/ml DNase1 and 8 U/ml papain (Sigma, St. Louis, MO). The samples were triturated after 15 and 30 minutes digestion. Enzymes were inactivated with addiion of 3 % FBS. Sample was washed twice with HBSS and then spun for 15 minutes at 1800 RPM at 4° C through 25% Percoll (GE HealthCare, Pittsburg, PA). The resulting fatty upper and fluid middle layers were removed from the pellet. The pellet was resuspended in 10ml of ice-cold HBSS and filtered through a 40 µm screen. Brain isolates were counted on a hemocytometer and viability was measured by Trypan blue exclusion.

**Enrichment of CD11b myeloid cells**

Cell isolates were washed in PBS, reconsituted in MACS buffer with 0.1% BSA (Miltenyi, Gladbach, Germany). Cells were counted and volume was adjusted for staining with non-human primate CD11b microbeads (Miltenyi, Gladbach, Germany). Forty million cells were reconstituted in 160µl of MACS buffer and reacted with 80 µl of

Accepted Manuscript Posted Online

Journal of Virology

JVI

Journal of Virology

Downloaded from http://jvi.asm.org/ on March 18, 2021 by guest

540 CD11b microbeads at 4°C for 15 minutes. After incubation, cells were washed with
541 MACS buffer with 0.1% BSA, reconstituted into 500 µl of MACS buffer and loaded onto
542 MACS Separator LD columns. Both the negative flow through and the positve CD11b+
543 cells were collected, cells were counted on Coulter Counter Z1. Isolates were used for
544 downstream processing and analyzed for epitope expression using FACS.

545 **Purification of alveolar macrophages from Bronchoalveolar lavage (BAL):** At
546 necropsy, the lung was lavaged with sterile saline and the BAL collected**.** Cells were
547 collected through centrifugation of the BAL at 250 g for 10 min at 4°C. The cell pellets
548 were washed twice with PBS containing 2% FBS and 2 mM EDTA. Cells were
549 resuspended in complete RPMI (composition described above) and used for
550 downstream applications.

551 **Isolation DNA/RNA from CD4+/CD11b+ cells:**

552 Enriched CD4+ T cells and CD11b+ macrophages were pelleted by centrifugation for 6
553 minutes at 1200 rpm and stored at -80°C until time of processing. To extract the
554 DNA/RNA from the cells, first the pellets were thawed on ice and thoroughly loosened
555 by flicking the tube. Then, 600 µl Buffer RLT Plus with 2-Mercaptoethanol (β-ME) at 10
556 µl/1 ml concentration was added and thoroughly mixed by vortexing. Following lysis, the
557 mixture was transferred to a QIAshredder (QIAGEN, Cat#79656) and the AllPrep
558 DNA/RNA Mini Kit (Qiagen, Cat#80204) was used for DNA/RNA isolation. The
559 remaining protocol followed was per the kit's instruction. RNA was eluted in 30 µl of
560 RNase free water after performing column DNase digestion while DNA was eluted in 50
561 µl of Elution Buffer provided in the kit. DNA/RNA concentrations were measured using

Accepted Manuscript Posted Online

Journal of Virology

JVI

Journal of Virology

Downloaded from http://jvi.asm.org/ on March 18, 2021 by guest

562 SimpliNano spectrophotometer (GE Healthcare Bio-Sciences Corp., Piscataway, NJ,
563 USA) and stored at -80°C deep freezer for future use.

564 **Isolation DNA/RNA from frozen tissues:**

565 For DNA/RNA isolation from tissues, the AllPrep DNA/RNA Mini Kit (QIAGEN
566 Germantown, MD, USA; Cat#80204) was used. Approximately 30 mg of frozen tissue
567 was placed into a 2 ml flat bottom centrifuge tube on dry ice with a 5 mm stainless steel
568 bead (QIAGEN Germantown, MD, USA; Cat#69989) at the bottom. Then, 600 µl buffer
569 RLT plus with 2-Mercaptoethanol (βME) at 10 µl βME/ml of RLT+ was added before
570 placing the tube into a TissueLyser LT (QIAGEN Germantown, MD, USA; Cat#69980)
571 set at 50 oscillations/second for 5 minutes. The lysate was checked for homogeneity
572 and transferred to a QIAshredder (QIAGEN Germantown, MD, USA; Cat#79656).
573 DNA/RNA was then isolated per the kit's instruction. RNA was eluted in 30 µl of RNase
574 free water after performing column DNase digestion, while DNA was eluted in 50 µl of
575 buffer EB. DNA/RNA concentrations were measured using SimpliNano
576 spectrophotometer (GE Healthcare Bio-Sciences Corp., Piscataway, NJ, USA) and
577 stored at -80°C deep freezer for future use.

578 **SIV cell associated RNA/DNA quantification:**

579 Total cell associated SIV RNA was quantified using RT-ddPCR using 100 nanogram of
580 RNA, 1-Step RT-ddPCR Advanced Kit for Probes (Bio-Rad; Cat#1864022) and same
581 set of primers and probe used for SIV plasma viral load quantification. ddPCR was
582 carried out on Bio-Rad QX200 AutoDG digital droplet PCR system. In brief, 22 ul of
583 reaction mix was used for droplet generation using QX200™ Droplet Generator, the

Accepted Manuscript Posted Online

Journal of Virology

JVI

Journal of Virology

Downloaded from http://jvi.asm.org/ on March 18, 2021 by guest

584 ddPCR plate having the emulsified samples was heat sealed with a foil (Bio-Rad;
585 Cat#181–4040) and amplified in a C1000 Touch thermal cycler (Bio-Rad, CA, USA).
586 After thermal cycling, ddPCR plates were transferred to the QX200 droplet reader (Bio-
587 Rad, CA, USA) for droplet count and fluorescence measurement. Positive droplets with
588 amplified products were separated from negative droplets without target amplicon by
589 applying a fluorescence amplitude threshold and the absolute quantity of RNA per
590 sample (copies/µl) was determined using QuantaSoft software. For quantification of cell
591 associated SIV DNA the same methodology was used as described above without
592 using the reverse transcription step and used 2X ddPCR Supermix for Probes (no
593 dUTP, Bio-rad; CA, USA; Cat#1863024) instead of 1-Step RT-ddPCR Advanced Kit.

594 **Tat/rev Induced Limiting Dilution Assay (TILDA):**

595 Tat/rev Induced Limiting Dilution Assay (TILDA) was performed as described earlier (86,
596 87). In brief, enriched CD4+ T cells from frozen PBMCs or LN total cells were
597 suspended in complete RPMI at 2 million cells/ml concentration, and then rested at
598 37ºC, 5% CO2 for a minimum of 2 hours. After resting, cells were divided into two
599 groups, one was stimulated with 100 ng/ml PMA and 1ug/ml ionomycin, and the other
600 group left untreated as control. After 16 hours, the cells were counted and then
601 centrifuged at 2000 rpm for 10 minutes to stop the reaction. Cells were then serially
602 diluted in complete RPMI to the following: 18,000, 9,000, 3,000, and 1,000 cells/ul. A
603 96-well PCR plate was divided column-wise in half for the two treatments, and then into
604 quarters for the four dilutions set in 8 replicates. In each well of the plate, 5 µl of Master
605 Mix was added and then 1 µl of the appropriate dilution for the corresponding treatment

Accepted Manuscript Posted Online

Journal of Virology

JVI

Journal of Virology

Downloaded from http://jvi.asm.org/ on March 18, 2021 by guest

606 was added to each well. The first PCR reaction mix contained 0.2 µl of Super Script III
607 RT/Platinum Taq Mix (Invitrogen; Cat# 2010520), 0.1 µl of Superase Rnase Inhibitor
608 (Invitrogen; Cat#00749138), 2.25 µl of Nuclease Free H2O (Ambion, Cat#AM9937), 2.2
609 µl of tris-EDTA (TE) Buffer, 0.125 µl of 10 µM SIVF (5' -
610 CACGAAAGAGAAGAAGAACTCCG – 3', IDT) and 0.125 ul 10 µM SIVR (5' -
611 TCTTTGCCTTCTCTGGTTGG – 3', IDT). To each well of the plate, 5 µl of reaction mix
612 was added. Pre-amplification settings included reverse transcription for 15 min at 50°C,
613 followed by denaturation for 2 min at 95°C, then 24 cycles of amplification at 95°C for 14
614 seconds and 60°C for 4 minutes. Pre-amplification was done in a LifePro Thermal
615 Cycler (Bioer Technology). After pre-amplification, 9 µl of qPCR reaction mix containing
616 5 ul LightCycler 480 Probes Master (Roche, Cat#04707494001), 3.4 ul of Nuclease
617 Free H2O (Ambion, AM9937), 0.2 µl of 20 µM Nested FW primer (5' -
618 AGGCTAAGGCTAATACATCTTCTG – 3', IDT), 0.2 µl of 20 µM SIVR (5' -
619 TCTTTGCCTTCTCTGGTTGG – 3', IDT), and 0.2 µl of 5 µM PROBE (5′-/56-
620 FAM/AAACCCATA/ZEN/TCCAACAGGACCCGG/3IABkFQ/-3′) details were added to
621 each well of a new 96-well PCR plate. Then, 1 µl of PCR product from pre-amplification
622 was added to the corresponding well in the new plate. Real-time PCR was performed in
623 QuantStudio 3 (Applied Biosystems, Waltham, MA, USA) with the following settings:
624 Pre-incubation at 95°C for 10 min, followed by 45 cycles at 95°C for 10 sec, 60°C for 30
625 sec, and 72°C for 1 sec, then finally a cooling period at 40°C for 30 sec.

626 **Intact proviral DNA assay (IPDA):**

Accepted Manuscript Posted Online

Journal of Virology

JVI

Journal of Virology

Downloaded from http://jvi.asm.org/ on March 18, 2021 by guest

Intact proviral DNA assay was performed as described by Bender et al.,(47) including thermal cycling conditions, primers and probes used in this assay. In brief, 250-1000 ng of DNA was mixed with 10 µl of 2X ddPCR Supermix for Probes (no dUTP, Bio-rad; Cat#1863024), 600 nM of primers and 200 nM of probes. ddPCR was carried out on Bio-Rad QX200 AutoDG digital droplet PCR system as described above. To quantify the input cell numbers, a parallel ddPCR reaction for rhesus macaque RPP30 gene was carried out.

**Macrophage Quantitative Viral Outgrowth Assay (MØ-QVOA):**

In this study, a modified version of macrophage (MØ-QVOA) was performed on CD11b+ macrophages isolated from brain, lung, and liver as described by Avalos et al., (52). In brief, cells were purified using a CD11b+ isolation kit per the manufacturer's recommended protocol (Miltenyi Biotec, Auburn, CA; cat# 130-091-100) as described above. The presence of the contaminating CD3+ T cells within the enriched CD11b+ cells was estimated by quantification of TCRβ as described by Avalos et al., (52). Prior to setting the culture, plates were coated with poly-L-lysine solution (Sigma, NC9778696) for 30 min and then washed twice with PBS. Purified cells were plated in triplicate and a 10-fold serial dilution in the presence of 10 µM zidovudine (Sigma), 25 nM DRV (Janssen), and 5 nM RTV (Merck). BrMφ media (Dulbecco's Modified Eagle Medium (DMEM) (Gibco; Cat#12491-015), 5% heat-inactivated FBS (Gibco; Cat#10437-028), 5% IS giant cell tumor conditioned media (Irvine Scientific; Cat#91006), 100 U/ml penicillin and 100 ug/ml strep (Gibco; Cat# 15140-122), 70 µg/ml gentamycin (Sigma Aldrich; Cat#G1397-10ML), 2 mM L-glutamine (Gibco; Cat#

Accepted Manuscript Posted Online

Journal of Virology

JVI

Journal of Virology

Downloaded from http://jvi.asm.org/ on March 18, 2021 by guest

35050079), 3 mM sodium pyruvate (Gibco; Cat#11360070) and 10 mM HEPES buffer (Gibco; Cat#35050079)) was used for brain cells and complete RPMI for lung and liver. The culture was then placed in a 37° C, 5% CO2 incubator for 72 hours to permit proper cell adherence. After the 3-day incubation, the antiretroviral-containing medium was removed and cells were washed with PBS (1X) and then replenished with BrMφ/complete RPMI media containing 10 ng/ml tumor necrosis factor alpha (TNF-α; ProSpec; Cat#CYT-114), 1 µg/ml Pam3csk4 (Sigma Aldrich; Cat# 506350), and 1 µg/ml prostaglandin (Sigma Aldrich; Cat#538904). Additionally, approximately $10^5$ CEMX-174 feeder cells were added to each well. Supernatants were collected on days 5, 7, 10, and 14 post-culture activation and replenished with activating agent's TNF-α, Pam3csk4, and Prostaglandin containing media. RNA was extracted from the supernatants using the QIAamp Viral RNA Mini Kit (QIAGEN, Cat#52906). Prior to extraction, the supernatants were centrifuged at 2000 rpm for 5 minutes, and then 140 µl was aliquoted and used per the kit's instruction to isolate RNA. The RNA was eluted in 50 µl of AVE buffer. Viral RNA was quantified in culture supernatant using RT-ddPCR as described above. The frequency of replication competent latent reservoir cells was estimated using the IUPMStats v1.0 infection frequency calculator (88).

**Flow cytometry evaluation of changes in T cell polarization in peripheral blood and lymph nodes**

The details of all fluorochrome-conjugated monoclonal antibodies used in the flow cytometry experiments are listed in Table 3. The single cell suspensions of PBMC and lymph nodes were prepared from samples collected from cART treated rhesus

Accepted Manuscript Posted Online

Journal of Virology

JVI

Journal of Virology

Downloaded from http://jvi.asm.org/ on March 18, 2021 by guest

671 macaques (n=11) during necropsy. 2-4 million of PBMCs were stimulated with
672 PMA/ionomycin at a final concentration of 50 ng/ml and 500 ng/ml respectively in
673 complete RPMI-1640 (composition described above). An unstimulated condition was
674 included as an experimental control. After 2 hours of incubation at 37°C in a humidified
675 5% CO2 incubator, 1 µl of GolgiPlug™ (BD Biosciences, USA; cat#555029) containing
676 brefeldin A was added to each well together with 1X of monensin (Biolegend, San
677 Diego, CA; cat#420701) and incubated for an additional 4 hours. After that 1:1000
678 dilution of zombie aqua amine reactive dye (Biolegend, San Diego, CA; cat# 423101)
679 was added to the cell suspensions and incubated for 30 minutes in the dark, cells were
680 washed and Fc blockade carried out using polyclonal anti-human Fc Receptor binding
681 inhibitor (eBioscienceTM, USA; Cat#16-9161-71). Surface staining was performed using
682 anti-CD45, anti-CD8, anti-CD4, and anti-NKG2A for panel 1 and using anti-CD25 and
683 anti-CD127 for panel 2 (Treg panel) and cells were incubated for 1 hour at room
684 temperature in dark. Thereafter for panel 1, cells were fixed using 2% paraformaldehyde
685 (PFA) solution for 30 minutes and permeabilization was performed using a 1X BD
686 perm/wash solution (BD Biosciences, USA; cat#554723) for 15 minutes at 4°C. Then,
687 anti-CD3, anti-IFNγ, anti-TNFα, and anti-IL-17 antibodies were added, and cells were
688 incubated at 4°C for 15 minutes, washed and resuspended in PBS. For the Treg panel,
689 fixation and permeabilization was performed using a 1X solution of Foxp3/Transcription
690 Factor Fix/Perm Concentrate (4X) (Tonbo Biosciences, San Diego, CA; Cat#TNB-1020-
691 L050) that was diluted using the 1X Foxp3/Transcription Factor Fix/Perm Diluent (Tonbo
692 Biosciences, San Diego, CA; Cat#TNB-1022-L160). Following this, anti-CD3, anti-IL-4

Accepted Manuscript Posted Online

Journal of Virology

JVI

Journal of Virology

Downloaded from http://jvi.asm.org/ on March 18, 2021 by guest

693 and anti-FOXP3 antibody were added and cells were incubated at 4°C for 15 minutes,
694 washed and resuspended in PBS.

695 For LN cell suspensions, 2-4 million cells were taken, and zombie UV viability dye was
696 added, and Fc receptor blockade performed as described above. Then, in the T cell
697 polarization panel, anti-CXCR5, anti-CXCR3, anti-CCR4, and anti-CCR6 antibodies
698 were added and in the Treg panel anti-CXCR5 antibody was added. After that cells in
699 both the panel was incubated at 370C for 30 minutes. Following this, ani-CD45, anti-
700 CD3, anti-CD4, anti-CD8, anti-CD20, anti-CD95, anti-CD38, anti-PD1, and anti-human
701 HLA-DR antibody were added in polarization panel. While in Treg panel, anti-CD25 and
702 anti-PD1 was added. After that, cells in both the panel were incubated at room
703 temperature for 30 minutes, washed and finally fixation was carried out. For the Treg
704 panel, intracellular staining was performed as described above for PBMC using anti-
705 FOXP3 and anti-CTLA4 antibodies. All events were acquired using the BD Fortessa
706 X450 and data analyzed using Flow Jo version 10.6. Flourescent minus one (FMO)
707 controls were included as cut offs for placement of gates when handling
708 nondiscriminatory variables.

709 **Statistical analysis**

710 Graph Pad Prism 8.0 software was used to carryout statistical comparisons and plot the
711 figures. Descriptive statistics were presented to summarize continuous variables.
712 Wilcoxon rank-sum tests were used to determine the statistically significant difference in
713 continuous outcomes between morphine and saline groups for flow cytometry data and

Accepted Manuscript Posted Online

other experimental data. All p values less than 0.05 are considered statistically significant.

## Acknowledgements:

We thank the staff and veterinarians of University of Nebraska Medical Center, Comparative Medicine department for housing and animal procedures. We also thank laboratory members of SNB, SB and HSF for helping in morphine and ART injections to rhesus macaques. We also acknowledge that antiretroviral drugs tenofovir alafenamide (TFV) and emtricitabine (FTC) were obtained from Gilead Sciences, Foster City, CA, USA, while dolutegravir (DTG) was procured from ViiV Healthcare, Research Triangle Park, NC, USA through research agreement. This study was supported by NIH grants R01DA043164, P30MH062261 to SNB, SB and HSF, and R01DA041751 to SNB and SB. The funders have no role in designing of the study and in interpretation of the results.



Journal of Virology

JVI

Journal of Virology

Downloaded from http://jvi.asm.org/ on March 18, 2021 by guest

Accepted Manuscript Posted Online

Journal of Virology

JVI

Journal of Virology

Downloaded from http://jvi.asm.org/ on March 18, 2021 by guest

## References:


1. Kreek MJ, Reed B, Butelman ER. 2019. Current status of opioid addiction treatment and related preclinical research. Sci Adv 5:eaax9140.
2. CDC. Assessing and Addressing Opioid Use Disorder (OUD).
3. Des Jarlais DC, Friedman SR, Novick DM, Sotheran JL, Thomas P, Yancovitz SR, Mildvan D, Weber J, Kreek MJ, Maslansky R. 1989. HIV-1 infection among intravenous drug users in Manhattan, New York City, from 1977 through 1987. JAMA 261:1008-12.
4. Degenhardt L, Peacock A, Colledge S, Leung J, Grebely J, Vickerman P, Stone J, Cunningham EB, Trickey A, Dumchev K, Lynskey M, Griffiths P, Mattick RP, Hickman M, Larney S. 2017. Global prevalence of injecting drug use and sociodemographic characteristics and prevalence of HIV, HBV, and HCV in people who inject drugs: a multistage systematic review. Lancet Glob Health 5:e1192-e1207.
5. Strang J, Volkow ND, Degenhardt L, Hickman M, Johnson K, Koob GF, Marshall BDL, Tyndall M, Walsh SL. 2020. Opioid use disorder. Nat Rev Dis Primers 6:3.
6. Roy S, Loh HH. 1996. Effects of opioids on the immune system. Neurochem Res 21:1375-86.
7. Roy S, Wang J, Kelschenbach J, Koodie L, Martin J. 2006. Modulation of immune function by morphine: implications for susceptibility to infection. J Neuroimmune Pharmacol 1:77-89.
8. Friedman H, Eisenstein TK. 2004. Neurological basis of drug dependence and its effects on the immune system. J Neuroimmunol 147:106-8.

Accepted Manuscript Posted Online

Journal of Virology

JVI

Journal of Virology

Downloaded from http://jvi.asm.org/ on March 18, 2021 by guest


759 9. Dinda A, Gitman M, Singhal PC. 2005. Immunomodulatory effect of morphine:
760 therapeutic implications. Expert Opin Drug Saf 4:669-75.
761 10. Nath A, Hauser KF, Wojna V, Booze RM, Maragos W, Prendergast M, Cass W,
762 Turchan JT. 2002. Molecular basis for interactions of HIV and drugs of abuse. J
763 Acquir Immune Defic Syndr 31 Suppl 2:S62-9.
764 11. Quaglio G, Lugoboni F, Talamini G, Lechi A, Mezzelani P. 2002. Prevalence of
765 tuberculosis infection and comparison of multiple-puncture liquid tuberculin test
766 and Mantoux test among drug users. Scand J Infect Dis 34:574-6.
767 12. Karagiannis TT, Cleary JP, Jr., Gok B, Henderson AJ, Martin NG, Yajima M,
768 Nelson EC, Cheng CS. 2020. Single cell transcriptomics reveals opioid usage
769 evokes widespread suppression of antiviral gene program. Nat Commun
770 11:2611.
771 13. Eisenstein TK. 2019. The Role of Opioid Receptors in Immune System Function.
772 Front Immunol 10:2904.
773 14. Vallejo R, de Leon-Casasola O, Benyamin R. 2004. Opioid therapy and
774 immunosuppression: a review. Am J Ther 11:354-65.
775 15. Smith DB, Simmonds P, Bell JE. 2014. Brain viral burden, neuroinflammation
776 and neurodegeneration in HAART-treated HIV positive injecting drug users. J
777 Neurovirol 20:28-38.
778 16. Bell JE, Arango JC, Anthony IC. 2006. Neurobiology of multiple insults: HIV-1-
779 associated brain disorders in those who use illicit drugs. J Neuroimmune
780 Pharmacol 1:182-91.

Accepted Manuscript Posted Online

Journal of Virology

JVI

Journal of Virology


781 17. Bell JE, Arango JC, Robertson R, Brettle RP, Leen C, Simmonds P. 2002. HIV
782 and drug misuse in the Edinburgh cohort. J Acquir Immune Defic Syndr 31 Suppl
783 2:S35-42.

784 18. Bokhari SM, Hegde R, Callen S, Yao H, Adany I, Li Q, Li Z, Pinson D, Yeh HW,
785 Cheney PD, Buch S. 2011. Morphine potentiates neuropathogenesis of SIV
786 infection in rhesus macaques. J Neuroimmune Pharmacol 6:626-39.

787 19. Jaureguiberry-Bravo M, Wilson R, Carvallo L, Berman JW. 2016. Opioids and
788 Opioid Maintenance Therapies: Their Impact on Monocyte-Mediated HIV
789 Neuropathogenesis. Curr HIV Res 14:417-430.

790 20. Hauser KF, Fitting S, Dever SM, Podhaizer EM, Knapp PE. 2012. Opiate drug
791 use and the pathophysiology of neuroAIDS. Curr HIV Res 10:435-52.

792 21. Guo CJ, Li Y, Tian S, Wang X, Douglas SD, Ho WZ. 2002. Morphine enhances
793 HIV infection of human blood mononuclear phagocytes through modulation of
794 beta-chemokines and CCR5 receptor. J Investig Med 50:435-42.

795 22. Kim S, Hahn YK, Podhaizer EM, McLane VD, Zou S, Hauser KF, Knapp PE.
796 2018. A central role for glial CCR5 in directing the neuropathological interactions
797 of HIV-1 Tat and opiates. J Neuroinflammation 15:285.

798 23. Murphy A, Barbaro J, Martinez-Aguado P, Chilunda V, Jaureguiberry-Bravo M,
799 Berman JW. 2019. The Effects of Opioids on HIV Neuropathogenesis. Front
800 Immunol 10:2445.

801 24. Li Y, Merrill JD, Mooney K, Song L, Wang X, Guo CJ, Savani RC, Metzger DS,
802 Douglas SD, Ho WZ. 2003. Morphine enhances HIV infection of neonatal
803 macrophages. Pediatr Res 54:282-8.




Downloaded from http://jvi.asm.org/ on March 18, 2021 by guest

Accepted Manuscript Posted Online

Journal of Virology

JVI

Journal of Virology


804 25. Mahajan SD, Schwartz SA, Aalinkeel R, Chawda RP, Sykes DE, Nair MP. 2005.
805 Morphine modulates chemokine gene regulation in normal human astrocytes.
806 Clin Immunol 115:323-32.
807 26. Zou S, Fitting S, Hahn YK, Welch SP, El-Hage N, Hauser KF, Knapp PE. 2011.
808 Morphine potentiates neurodegenerative effects of HIV-1 Tat through actions at
809 mu-opioid receptor-expressing glia. Brain 134:3616-31.
810 27. Dave RS, Ali H, Sil S, Knight LA, Pandey K, Madduri LSV, Qiu F, Ranga U, Buch
811 S, Byrareddy SN. 2020. NF-κB Duplications in the Promoter-Variant HIV-1C LTR
812 Impact Inflammation Without Altering Viral Replication in the Context of Simian
813 Human Immunodeficiency Viruses and Opioid-Exposure. Front Immunol 11:95.
814 28. Ndung'u T, McCune JM, Deeks SG. 2019. Why and where an HIV cure is
815 needed and how it might be achieved. Nature 576:397-405.
816 29. Vanhamel J, Bruggemans A, Debyser Z. 2019. Establishment of latent HIV-1
817 reservoirs: what do we really know? J Virus Erad 5:3-9.
818 30. Massanella M, Richman DD. 2016. Measuring the latent reservoir in vivo. J Clin
819 Invest 126:464-72.
820 31. Castro-Gonzalez S, Colomer-Lluch M, Serra-Moreno R. 2018. Barriers for HIV
821 Cure: The Latent Reservoir. AIDS Res Hum Retroviruses 34:739-759.
822 32. Lorenzo-Redondo R, Fryer HR, Bedford T, Kim EY, Archer J, Pond SLK, Chung
823 YS, Penugonda S, Chipman J, Fletcher CV, Schacker TW, Malim MH, Rambaut
824 A, Haase AT, McLean AR, Wolinsky SM. 2016. Persistent HIV-1 replication
825 maintains the tissue reservoir during therapy. Nature 530:51-56.




Downloaded from http://jvi.asm.org/ on March 18, 2021 by guest

Accepted Manuscript Posted Online

Journal of Virology

JVI

Journal of Virology

Downloaded from http://jvi.asm.org/ on March 18, 2021 by guest

826 33. Deleage C, Wietgrefe SW, Del Prete G, Morcock DR, Hao XP, Piatak M, Jr.,
827 Bess J, Anderson JL, Perkey KE, Reilly C, McCune JM, Haase AT, Lifson JD,
828 Schacker TW, Estes JD. 2016. Defining HIV and SIV Reservoirs in Lymphoid
829 Tissues. Pathog Immun 1:68-106.
830 34. Abreu C, Shirk EN, Queen SE, Beck SE, Mangus LM, Pate KAM, Mankowski JL,
831 Gama L, Clements JE. 2019. Brain macrophages harbor latent, infectious simian
832 immunodeficiency virus. AIDS 33 Suppl 2:S181-S188.
833 35. Kruize Z, Kootstra NA. 2019. The Role of Macrophages in HIV-1 Persistence and
834 Pathogenesis. Front Microbiol 10:2828.
835 36. Wong JK, Yukl SA. 2016. Tissue reservoirs of HIV. Curr Opin HIV AIDS 11:362-
836 70.
837 37. Roy S, Ninkovic J, Banerjee S, Charboneau RG, Das S, Dutta R, Kirchner VA,
838 Koodie L, Ma J, Meng J, Barke RA. 2011. Opioid drug abuse and modulation of
839 immune function: consequences in the susceptibility to opportunistic infections. J
840 Neuroimmune Pharmacol 6:442-65.
841 38. Gao M, Sun J, Jin W, Qian Y. 2012. Morphine, but not ketamine, decreases the
842 ratio of Th1/Th2 in CD4-positive cells through T-bet and GATA3. Inflammation
843 35:1069-77.
844 39. Meng J, Yu H, Ma J, Wang J, Banerjee S, Charboneau R, Barke RA, Roy S.
845 2013. Morphine induces bacterial translocation in mice by compromising
846 intestinal barrier function in a TLR-dependent manner. PLoS One 8:e54040.
847 40. Hutchinson MR, Zhang Y, Shridhar M, Evans JH, Buchanan MM, Zhao TX,
848 Slivka PF, Coats BD, Rezvani N, Wieseler J, Hughes TS, Landgraf KE, Chan S,

Accepted Manuscript Posted Online

849 Fong S, Phipps S, Falke JJ, Leinwand LA, Maier SF, Yin H, Rice KC, Watkins
850 LR. 2010. Evidence that opioids may have toll-like receptor 4 and MD-2 effects.
851 Brain Behav Immun 24:83-95.
852 41. Hutchinson MR, Zhang Y, Brown K, Coats BD, Shridhar M, Sholar PW, Patel SJ,
853 Crysdale NY, Harrison JA, Maier SF, Rice KC, Watkins LR. 2008. Non-
854 stereoselective reversal of neuropathic pain by naloxone and naltrexone:
855 involvement of toll-like receptor 4 (TLR4). Eur J Neurosci 28:20-9.
856 42. Hutchinson MR, Northcutt AL, Hiranita T, Wang X, Lewis SS, Thomas J, van
857 Steeg K, Kopajtic TA, Loram LC, Sfregola C, Galer E, Miles NE, Bland ST, Amat
858 J, Rozeske RR, Maslanik T, Chapman TR, Strand KA, Fleshner M, Bachtell RK,
859 Somogyi AA, Yin H, Katz JL, Rice KC, Maier SF, Watkins LR. 2012. Opioid
860 activation of toll-like receptor 4 contributes to drug reinforcement. J Neurosci
861 32:11187-200.
862 43. Due MR, Piekarz AD, Wilson N, Feldman P, Ripsch MS, Chavez S, Yin H,
863 Khanna R, White FA. 2012. Neuroexcitatory effects of morphine-3-glucuronide
864 are dependent on Toll-like receptor 4 signaling. J Neuroinflammation 9:200.
865 44. Wang Y, Wang X, Ye L, Li J, Song L, Fulambarkar N, Ho W. 2012. Morphine
866 suppresses IFN signaling pathway and enhances AIDS virus infection. PLoS One
867 7:e31167.
868 45. Bell JE, Brettle RP, Chiswick A, Simmonds P. 1998. HIV encephalitis, proviral
869 load and dementia in drug users and homosexuals with AIDS. Effect of
870 neocortical involvement. Brain 121 ( Pt 11):2043-52.



Journal of Virology
JVI
Journal of Virology
Downloaded from http://jvi.asm.org/ on March 18, 2021 by guest

Accepted Manuscript Posted Online

871 46. Bruner KM, Wang Z, Simonetti FR, Bender AM, Kwon KJ, Sengupta S, Fray EJ,
872 Beg SA, Antar AAR, Jenike KM, Bertagnolli LN, Capoferri AA, Kufera JT,
873 Timmons A, Nobles C, Gregg J, Wada N, Ho YC, Zhang H, Margolick JB,
874 Blankson JN, Deeks SG, Bushman FD, Siliciano JD, Laird GM, Siliciano RF.
875 2019. A quantitative approach for measuring the reservoir of latent HIV-1
876 proviruses. Nature 566:120-125.
877 47. Bender AM, Simonetti FR, Kumar MR, Fray EJ, Bruner KM, Timmons AE, Tai
878 KY, Jenike KM, Antar AAR, Liu PT, Ho YC, Raugi DN, Seydi M, Gottlieb GS,
879 Okoye AA, Del Prete GQ, Picker LJ, Mankowski JL, Lifson JD, Siliciano JD, Laird
880 GM, Barouch DH, Clements JE, Siliciano RF. 2019. The Landscape of Persistent
881 Viral Genomes in ART-Treated SIV, SHIV, and HIV-2 Infections. Cell Host
882 Microbe 26:73-85 e4.
883 48. Lee GQ, Orlova-Fink N, Einkauf K, Chowdhury FZ, Sun X, Harrington S, Kuo HH,
884 Hua S, Chen HR, Ouyang Z, Reddy K, Dong K, Ndung'u T, Walker BD,
885 Rosenberg ES, Yu XG, Lichterfeld M. 2017. Clonal expansion of genome-intact
886 HIV-1 in functionally polarized Th1 CD4+ T cells. J Clin Invest 127:2689-2696.
887 49. Amancha PK, Ackerley CG, Duphare C, Lee M, Hu YJ, Amara RR, Kelley CF.
888 2019. Distribution of Functional CD4 and CD8 T cell Subsets in Blood and Rectal
889 Mucosal Tissues. Sci Rep 9:6951.
890 50. Velu V, Mylvaganam G, Ibegbu C, Amara RR. 2018. Tfh1 Cells in Germinal
891 Centers During Chronic HIV/SIV Infection. Front Immunol 9:1272.
892 51. Gosselin A, Wiche Salinas TR, Planas D, Wacleche VS, Zhang Y, Fromentin R,
893 Chomont N, Cohen EA, Shacklett B, Mehraj V, Ghali MP, Routy JP, Ancuta P.



Journal of Virology
JVI
Journal of Virology
Downloaded from http://jvi.asm.org/ on March 18, 2021 by guest

Accepted Manuscript Posted Online

894 2017. HIV persists in CCR6+CD4+ T cells from colon and blood during
895 antiretroviral therapy. AIDS 31:35-48.
896 52. Avalos CR, Price SL, Forsyth ER, Pin JN, Shirk EN, Bullock BT, Queen SE, Li M,
897 Gellerup D, O'Connor SL, Zink MC, Mankowski JL, Gama L, Clements JE. 2016.
898 Quantitation of Productively Infected Monocytes and Macrophages of Simian
899 Immunodeficiency Virus-Infected Macaques. J Virol 90:5643-5656.
900 53. Campbell JH, Hearps AC, Martin GE, Williams KC, Crowe SM. 2014. The
901 importance of monocytes and macrophages in HIV pathogenesis, treatment, and
902 cure. AIDS 28:2175-87.
903 54. Spudich S, Clements JE. 2019. HIV persistence in the central nervous system
904 during antiretroviral therapy: evidence and implications. AIDS 33 Suppl 2:S103-
905 S106.
906 55. Veenhuis RT, Clements JE, Gama L. 2019. HIV Eradication Strategies:
907 Implications for the Central Nervous System. Curr HIV/AIDS Rep 16:96-104.
908 56. Wang X, Ma TC, Li JL, Zhou Y, Geller EB, Adler MW, Peng JS, Zhou W, Zhou
909 DJ, Ho WZ. 2015. Heroin inhibits HIV-restriction miRNAs and enhances HIV
910 infection of macrophages. Front Microbiol 6:1230.
911 57. Reynolds JL, Law WC, Mahajan SD, Aalinkeel R, Nair B, Sykes DE, Mammen
912 MJ, Yong KT, Hui R, Prasad PN, Schwartz SA. 2012. Morphine and galectin-1
913 modulate HIV-1 infection of human monocyte-derived macrophages. J Immunol
914 188:3757-65.



Journal of Virology
JVI
Journal of Virology
Downloaded from http://jvi.asm.org/ on March 18, 2021 by guest

Accepted Manuscript Posted Online

Journal of Virology

JVI

Journal of Virology

915 58. Bixby JG, Laur O, Johnson WE, Desrosiers RC. 2010. Diversity of envelope
916 genes from an uncloned stock of SIVmac251. AIDS Res Hum Retroviruses
917 26:1115-31.
918 59. Bar KJ, Li H, Chamberland A, Tremblay C, Routy JP, Grayson T, Sun C, Wang
919 S, Learn GH, Morgan CJ, Schumacher JE, Haynes BF, Keele BF, Hahn BH,
920 Shaw GM. 2010. Wide variation in the multiplicity of HIV-1 infection among
921 injection drug users. J Virol 84:6241-7.
922 60. Abreu CM, Veenhuis RT, Avalos CR, Graham S, Parrilla DR, Ferreira EA, Queen
923 SE, Shirk EN, Bullock BT, Li M, Metcalf Pate KA, Beck SE, Mangus LM,
924 Mankowski JL, Mac Gabhann F, O'Connor SL, Gama L, Clements JE. 2019.
925 Myeloid and CD4 T Cells Comprise the Latent Reservoir in Antiretroviral
926 Therapy-Suppressed SIVmac251-Infected Macaques. mBio 10.
927 61. Berkowitz BA. 1976. The relationship of pharmacokinetics to pharmacological
928 activity: morphine, methadone and naloxone. Clin Pharmacokinet 1:219-30.
929 62. Kumar R, Orsoni S, Norman L, Verma AS, Tirado G, Giavedoni LD, Staprans S,
930 Miller GM, Buch SJ, Kumar A. 2006. Chronic morphine exposure causes
931 pronounced virus replication in cerebral compartment and accelerated onset of
932 AIDS in SIV/SHIV-infected Indian rhesus macaques. Virology 354:192-206.
933 63. Kulpa DA, Chomont N. 2015. HIV persistence in the setting of antiretroviral
934 therapy: when, where and how does HIV hide? J Virus Erad 1:59-66.
935 64. Banga R, Procopio FA, Noto A, Pollakis G, Cavassini M, Ohmiti K, Corpataux
936 JM, de Leval L, Pantaleo G, Perreau M. 2016. PD-1(+) and follicular helper T



Downloaded from http://jvi.asm.org/ on March 18, 2021 by guest

Accepted Manuscript Posted Online

937 cells are responsible for persistent HIV-1 transcription in treated aviremic
938 individuals. Nat Med 22:754-61.
939 65. Petrovas C, Yamamoto T, Gerner MY, Boswell KL, Wloka K, Smith EC,
940 Ambrozak DR, Sandler NG, Timmer KJ, Sun X, Pan L, Poholek A, Rao SS,
941 Brenchley JM, Alam SM, Tomaras GD, Roederer M, Douek DC, Seder RA,
942 Germain RN, Haddad EK, Koup RA. 2012. CD4 T follicular helper cell dynamics
943 during SIV infection. J Clin Invest 122:3281-94.
944 66. Xu H, Wang X, Malam N, Aye PP, Alvarez X, Lackner AA, Veazey RS. 2016.
945 Persistent Simian Immunodeficiency Virus Infection Drives Differentiation,
946 Aberrant Accumulation, and Latent Infection of Germinal Center Follicular T
947 Helper Cells. J Virol 90:1578-87.
948 67. Zhang EY, Xiong J, Parker BL, Chen AY, Fields PE, Ma X, Qiu J, Yankee TM.
949 2011. Depletion and recovery of lymphoid subsets following morphine
950 administration. Br J Pharmacol 164:1829-44.
951 68. Vojdani Z, Dehghani F, Seyedi F, Noorafshan A, Baha-al-din Bagi F. 2010.
952 Quantitative study of the effects of morphine on the mouse spleen and inguinal
953 lymph node. Arch Iran Med 13:294-300.
954 69. Brown JN, Ortiz GM, Angel TE, Jacobs JM, Gritsenko M, Chan EY, Purdy DE,
955 Murnane RD, Larsen K, Palermo RE, Shukla AK, Clauss TR, Katze MG, McCune
956 JM, Smith RD. 2012. Morphine produces immunosuppressive effects in
957 nonhuman primates at the proteomic and cellular levels. Mol Cell Proteomics
958 11:605-18.



Journal of Virology
JVI
Journal of Virology
Downloaded from http://jvi.asm.org/ on March 18, 2021 by guest

Accepted Manuscript Posted Online

959 70. Macatangay BJ, Rinaldo CR. 2010. Regulatory T cells in HIV immunotherapy.
960 HIV Ther 4:639-647.
961 71. Banga R, Procopio FA, Ruggiero A, Noto A, Ohmiti K, Cavassini M, Corpataux J-
962 M, Paxton WA, Pollakis G, Perreau M. 2018. Blood CXCR3(+) CD4 T Cells Are
963 Enriched in Inducible Replication Competent HIV in Aviremic Antiretroviral
964 Therapy-Treated Individuals. Frontiers in immunology 9:144-144.
965 72. Velu V, Mylvaganam GH, Gangadhara S, Hong JJ, Iyer SS, Gumber S, Ibegbu
966 CC, Villinger F, Amara RR. 2016. Induction of Th1-biased T follicular helper (Tfh)
967 cells in lymphoid tissues during chronic simian immunodeficiency virus infection
968 defines functionally distinct germinal center Tfh cells. The Journal of Immunology
969 197:1832-1842.
970 73. Velu V, Mylvaganam G, Ibegbu C, Amara RR. 2018. Tfh1 Cells in Germinal
971 Centers During Chronic HIV/SIV Infection. Frontiers in Immunology 9.
972 74. Wang X, Liu J, Zhou L, Ho WZ. 2019. Morphine Withdrawal Enhances HIV
973 Infection of Macrophages. Front Immunol 10:2601.
974 75. Leibrand CR, Paris JJ, Jones AM, Masuda QN, Halquist MS, Kim WK, Knapp
975 PE, Kashuba ADM, Hauser KF, McRae M. 2019. HIV-1 Tat and opioids act
976 independently to limit antiretroviral brain concentrations and reduce blood-brain
977 barrier integrity. J Neurovirol 25:560-577.
978 76. Mahajan SD, Aalinkeel R, Sykes DE, Reynolds JL, Bindukumar B, Fernandez
979 SF, Chawda R, Shanahan TC, Schwartz SA. 2008. Tight junction regulation by
980 morphine and HIV-1 tat modulates blood-brain barrier permeability. J Clin
981 Immunol 28:528-41.



Journal of Virology
JVI
Journal of Virology
Downloaded from http://jvi.asm.org/ on March 18, 2021 by guest

Accepted Manuscript Posted Online

Journal of Virology

JVI

Journal of Virology

Downloaded from http://jvi.asm.org/ on March 18, 2021 by guest

982 77. Liu WY, Wang ZB, Zhang LC, Wei X, Li L. 2012. Tight junction in blood-brain
983 barrier: an overview of structure, regulation, and regulator substances. CNS
984 Neurosci Ther 18:609-15.
985 78. Strazza M, Pirrone V, Wigdahl B, Dampier W, Lin W, Feng R, Maubert ME,
986 Weksler B, Romero IA, Couraud PO, Nonnemacher MR. 2016. Prolonged
987 Morphine Exposure Induces Increased Firm Adhesion in an in Vitro Model of the
988 Blood-Brain Barrier. Int J Mol Sci 17.
989 79. Wang X, Ye L, Zhou Y, Liu MQ, Zhou DJ, Ho WZ. 2011. Inhibition of anti-HIV
990 microRNA expression: a mechanism for opioid-mediated enhancement of HIV
991 infection of monocytes. Am J Pathol 178:41-7.
992 80. Purohit V, Rapaka RS, Rutter J, Shurtleff D. 2012. Do opioids activate latent HIV-
993 1 by down-regulating anti-HIV microRNAs? J Neuroimmune Pharmacol 7:519-23.
994 81. Sakane N, Kwon HS, Pagans S, Kaehlcke K, Mizusawa Y, Kamada M, Lassen
995 KG, Chan J, Greene WC, Schnoelzer M, Ott M. 2011. Activation of HIV
996 transcription by the viral Tat protein requires a demethylation step mediated by
997 lysine-specific demethylase 1 (LSD1/KDM1). PLoS Pathog 7:e1002184.
998 82. Llewellyn GN, Alvarez-Carbonell D, Chateau M, Karn J, Cannon PM. 2018. HIV-
999 1 infection of microglial cells in a reconstituted humanized mouse model and
1000 identification of compounds that selectively reverse HIV latency. J Neurovirol
1001 24:192-203.
1002 83. Miyagi T, Chuang LF, Doi RH, Carlos MP, Torres JV, Chuang RY. 2000.
1003 Morphine induces gene expression of CCR5 in human CEMx174 lymphocytes. J
1004 Biol Chem 275:31305-10.

Accepted Manuscript Posted Online

Journal of Virology

JVI

Journal of Virology

Downloaded from http://jvi.asm.org/ on March 18, 2021 by guest

1005 84. Byrareddy SN, Kallam B, Arthos J, Cicala C, Nawaz F, Hiatt J, Kersh EN,
1006 McNicholl JM, Hanson D, Reimann KA, Brameier M, Walter L, Rogers K, Mayne
1007 AE, Dunbar P, Villinger T, Little D, Parslow TG, Santangelo PJ, Villinger F, Fauci
1008 AS, Ansari AA. 2014. Targeting alpha4beta7 integrin reduces mucosal
1009 transmission of simian immunodeficiency virus and protects gut-associated
1010 lymphoid tissue from infection. Nat Med 20:1397-400.
1011 85. Marcondes MC, Burudi EM, Huitron-Resendiz S, Sanchez-Alavez M, Watry D,
1012 Zandonatti M, Henriksen SJ, Fox HS. 2001. Highly activated CD8(+) T cells in
1013 the brain correlate with early central nervous system dysfunction in simian
1014 immunodeficiency virus infection. J Immunol 167:5429-38.
1015 86. Frank I, Acharya A, Routhu NK, Aravantinou M, Harper JL, Maldonado S, Sole
1016 Cigoli M, Semova S, Mazel S, Paiardini M, Derby N, Byrareddy SN, Martinelli E.
1017 2019. A Tat/Rev Induced Limiting Dilution Assay to Measure Viral Reservoirs in
1018 Non-Human Primate Models of HIV Infection. Sci Rep 9:12078.
1019 87. Olwenyi OA, Acharya A, Routhu NK, Pierzchalski K, Jones JW, Kane MA, Sidell
1020 N, Mohan M, Byrareddy SN. 2020. Retinoic Acid Improves the Recovery of
1021 Replication-Competent Virus from Latent SIV Infected Cells. Cells 9.
1022 88. Rosenbloom DI, Elliott O, Hill AL, Henrich TJ, Siliciano JM, Siliciano RF. 2015.
1023 Designing and Interpreting Limiting Dilution Assays: General Principles and
1024 Applications to the Latent Reservoir for Human Immunodeficiency Virus-1. Open
1025 Forum Infect Dis 2:ofv123.

1026

1027

Accepted Manuscript Posted Online

Journal of Virology

JVI

Journal of Virology

Downloaded from http://jvi.asm.org/ on March 18, 2021 by guest

## Figure legends

**Figure 1: Experimental schema utilized for the study.** The study included a total of 19 rhesus macaques. The study had two experimental arms, one of which contain eight monkeys that did not received antiretroviral therapy (A) and the other group had eleven macaques those were treated with combinational antiretroviral therapy (B). (A) In this group out of eight animals four were ramp up with 6 mg/kg intramuscular injection of morphine twice daily for two weeks and then continue morphine dose for seven weeks and the other four animals received similar dose of normal saline (control group). After nine weeks all the macaques were intravenously infected with 200TCID50 of SIVmac251 while the administration of morphine/saline continued until end of the study. (B) In this group out of eleven animals six were ramp up with 6 mg/kg intramuscular injection of morphine twice daily for two weeks and then continue morphine dose for seven weeks and the other five animals received similar dose of normal saline (control group). After nine weeks all the macaques were intravenously infected with 200TCID50 of SIVmac251. Five weeks post infection, anti-retroviral therapy (ART) was initiated and continued until end of the study. ART regimen consisted of two reverse transcriptase inhibitors (FTC: 40 mg/ml and TFV: 20 mg/ml) and one integrase inhibitor (DTG: 2.5 mg/ml). The anti-retroviral drugs were administered subcutaneously once daily at 1

Accepted Manuscript Posted Online

Journal of Virology

JVI

Journal of Virology

Downloaded from http://jvi.asm.org/ on March 18, 2021 by guest

1050 ml/kg body weight, while the administration of morphine/saline continued until end of the
1051 study.
1052
1053 **Figure 2: Plasma and CSF viral load of morphine administered SIVmac251**
1054 **infected *rhesus macaques*.** Ten macaques were ramp-up with daily twice dose of
1055 morphine (6 mg/kg) for eight weeks and nine macaques were served as control
1056 (received saline), then infected with SIVmac251. Five weeks post infection, in six
1057 animals from morphine group and five animals from control group daily single dose of
1058 combination antiretroviral therapy (cART) was initiated. Daily dose of cART and
1059 morphine/saline administration continued until the end of the study. Plasma and CSF
1060 SIV viral load was measured longitudinally in all *rhesus macaques* using quantitative
1061 PCR (QPCR) assay. **(A)** Longitudinal plasma viral loads of individual animals that did
1062 not receive cART (copies/ml); **(B)** Longitudinal CSF viral loads of individual animals that
1063 did not received cART (copies/ml); **(C)** Geometric mean of plasma viral loads of animals
1064 that did not received cART (black line represents control group who received saline and
1065 red line represents morphine treated group); **(D)** Geometric mean of CSF viral loads
1066 animals that did not received cART (black line represents control group who received
1067 saline and red line represents morphine treated group). **(E)** Longitudinal plasma viral
1068 loads of individual animals received cART (copies/ml); **(F)** Longitudinal CSF viral loads
1069 of individual animals received cART (copies/ml); **(G)** Geometric mean of plasma viral
1070 loads of animals received cART (black line represents control group who received
1071 saline and red line represents morphine treated group); **(H)** Geometric mean of CSF
1072 viral loads animals received cART (black line represents control group who received

Accepted Manuscript Posted Online

Journal of Virology

JVI

Journal of Virology

Downloaded from http://jvi.asm.org/ on March 18, 2021 by guest

1073 saline and red line represents morphine treated group). The shaded region indicates
1074 ART phase of the study. The dashed lines represent limit of detection of the assay (50
1075 copies/ml).
1076
1077 **Figure 3: Cell associated SIV DNA and RNA level in different tissue compartments**
1078 **between morphine administered versus control groups of SIVmac251 infected**
1079 ***rhesus maca*ques. (A)** SIV DNA copies per million CD4+ T cells isolated from
1080 peripheral blood mononuclear cells; **(B)** SIV RNA copies per million CD4+ T cells
1081 isolated from peripheral blood mononuclear cells; (**C)** SIV DNA copies per million CD4+
1082 T cells isolated from lymph node (LN) cells; **(D)** SIV RNA copies per million CD4+ T
1083 cells isolated from LN cells; **(E)** SIV DNA copies per million cells from rectal mucosal
1084 tissue; **(F)** SIV RNA copies per million cells from rectal mucosal tissue; The green dots
1085 represent samples from control animals administered saline that did not received ART,
1086 maroon dots represent samples from morphine administered animals that did not
1087 received ART, blue dots represent samples from control animals administered saline
1088 and treated with ART and the red dots represent samples from morphine administered
1089 animals treated with ART. The horizontal dashed lines represent limit of detection of the
1090 assay (20 copies/ml). All values below limit of detection are bringing to the limit of
1091 detection for better representation in the figure.
1092
1093 **Figure 4: Cell associated SIV DNA and RNA level in spleen and lung in morphine**
1094 **administered versus control group of SIVmac251 infected *rhesus maca*ques. (A)**
1095 SIV DNA copies per million cells from spleen; **(B)** SIV RNA copies per million cells from

Accepted Manuscript Posted Online

Journal of Virology

JVI

Journal of Virology

Downloaded from http://jvi.asm.org/ on March 18, 2021 by guest

spleen; (**C)** SIV DNA copies per million alveolar macrophages from lung; **(D)** SIV RNA copies per million alveolar macrophages from lung; The green dots represent samples from control animals administered saline that did not received ART, maroon dots represent samples from morphine administered animals that did not received ART, blue dots represent samples from control animals administered saline and treated with ART and the red dots represent samples from morphine administered animals treated with ART. The horizontal dashed lines represent limit of detection of the assay (20 copies/ml). All values bellow limit of detection are bringing to the limit of detection for better representation in the figure.

**Figure 5: Size of SIV reservoirs in CD4+ T cells from peripheral blood and lymph nodes (LNs) in morphine administered versus control group of SIVmac251 infected ART suppressed *rhesus maca*ques. (A, B)** Size of inducible SIV latent reservoirs in CD4+ T cells from peripheral blood and LNs of morphine administered and control rhesus macaques received saline were measured by Tat/rev Induced Limiting Dilution Assay (TILDA) which quantify frequency of CD4+ T cells producing inducible ms-Tat/rev transcript per million of CD4+ T cells. **(C, D)** Frequency of intact SIV genome in CD4+ T cells isolated from blood and LNs of morphine/saline administered, SIVmac251 infected cART treated rhesus macaques were quantified using IPDA.

**Figure 6: Gating strategy for CD4+ Th1/Th17 polarity in PBMCs.** Briefly, CD45+ cells were gated and later NKT cells excluded from the total CD3+ T cell pool. CD4 and CD8 T cells were gated out of the total T cells. The CD4 T cells were then further

Accepted Manuscript Posted Online

Journal of Virology

JVI

Journal of Virology

Downloaded from http://jvi.asm.org/ on March 18, 2021 by guest

1119 investigated to determine the extent of IFNγ, TNFα and IL-17 cytokine secretion
1120 following PMA and ionomycin stimulation.
1121
1122 **Figure 7: Gating strategy for Th2/T regs in PBMCs.** Dead cells excluded based on
1123 zombie UV dye positive expression. Based on FSC-A vs SSC-A gating, lymphocytes
1124 were later gated and CD4+ T cells further obtained from total CD3+ T cells. From the
1125 CD4+ T cells, the extent of IL-4 cytokine secretion was then evaluated following
1126 stimulation with PMA/ ionomycin. Finally, the frequencies of CD4+ T regs were
1127 evaluated based on the expression of CD25+ and CD127-. These cells were later
1128 evaluated for their expression of the transcription factor of FoxP3+ to give the final
1129 frequency of T regs denoted as %CD4+ CD25+ CD127- Foxp3+ cells.
1130
1131 **Figure 8: Gating strategy for Lymph node activation and Tfh Polarization panel.**
1132 CD45+ leukocytes were gated and T and non- T lymphocytes discriminated based on
1133 CD3+ expression. CD3- cells were segregated based on CD20+ (B cells) and CD8α+
1134 (NK cells). The activation profiles of these cells were further evaluated based on CD38+
1135 and HLA-DR+ co-expression. CD4+ T cells were separately gated out of CD3+ T cells
1136 and levels of activation determined. The CD95+ memory cell marker was then included
1137 to obtain memory CD4+ T cells and later delineate the Tfh population based on CXCR5
1138 and PD-1. Additional chemokines were used to study Tfh polarity based on Tfh1
1139 (CXCR3), Tfh2 (CCR4), Tfh17 (CCR6) and T follicular regulatory cells (CD25 and
1140 FoxP3).
1141

Accepted Manuscript Posted Online

Journal of Virology

JVI

Journal of Virology

Downloaded from http://jvi.asm.org/ on March 18, 2021 by guest

**Figure 9: Immune dynamics in peripheral blood and lymph node compartments in morphine administered versus saline (control) groups of cART treated SIV mac 251 infected rhesus macaques.** Following stimulation with PMA/ ionomycin, differences in the levels of: (A) PBMC CD4+ Th1 cells secreting IFNγ; (B) PBMC CD4+ Th1 cells secreting TNFα; (C) PBMC CD4+ Th2 cells secreting IL-4; (D) PBMC CD4+ Th17 cells secreting IL-17; (E) PBMC Tregs were also outlined as CD25+FoxP3+CD4+ T cells; Within the lymph nodes, the frequencies of (F) T follicular helper (Tfh) cells based on CD95+PD-1+ co-expression amongst CXCR5+ T cells were assessed. (G) Similarly, the levels of T follicular regulatory cells (Tfr) were evaluated based on CD25+ and FoxP3+ co-expression amongst the Tfh population. (H) Simultaneous evaluation of T regs (CD25+ and FoxP3+) within the CXCR5- CD4+ T cell population was also carried out. (I) Representation of Tfh polarity as delineated as Tfh1, Tfh 17 and Tfh 2 based on the surface expression of specific chemokine receptors. Collectively, (J) Tfh1 were based on CXCR3 (K) Tfh17 based on extent of CCR6 and (L)Tfh2 based on CCR4 expression amongst CXCR5 hi PD-1 hi Tfh cells. (M) Representation of CD4+ T cell activation in one experimental and one control sample. (N) Levels of CD4+ T cell (O) B cell and (P) NK cell activation as measured by the extent of CD38 and HLA-DR co-expression.

**Figure 10:** Gating strategy to detect the purity of CD11b+ macrophages isolated from brain of rhesus macaques as described. Briefly, comparisons in the subsequent purity of CD11B microglia showed that higher yields of brain macrophages were obtained following enrichment of brain cells with CD11B beads.

Accepted Manuscript Posted Online

Journal of Virology

JVI

Journal of Virology

Downloaded from http://jvi.asm.org/ on March 18, 2021 by guest

**Figure 11: Size of SIV reservoirs in CD11b+ macrophages from brain of morphine administered versus control group of SIVmac251 infected ART suppressed *rhesus maca*ques. (A)** SIV DNA copies per million CD11b+ macrophages isolated from brain of morphine administered and control rhesus macaques received saline; **(B)** SIV RNA copies per million CD11b+ macrophages isolated from brain of morphine administered and control rhesus macaques received saline. **(C)** Size of functional latent reservoirs estimated by macrophage quantitative viral outgrowth assay (MØ-QVOA) in CD11b+ positive macrophages purified from brain of morphine administered and control rhesus macaques received saline. Infectious unites per million cells (IUPM) were estimated using the IUPMStats v1.0 infection frequency calculator. All values below limit of detection are bringing to the limit of detection for better representation in the figure.

**Figure 12: Proposed mechanism of morphine mediated differential regulation of SIV reservoirs in lymphoid tissue versus myeloid cells in CNS. (A)** Chronic morphine exposure leads to a reduction of Tfh cells in lymph nodes (LNs) which serves as the major HIV/SIV reservoirs in LNs. This may be responsible for observing reduction in SIV reservoirs in our morphine dependent, SIVmac251 infected cART treated *rhesus macaque* model. **(B)** Chronic morphine exposure increases the permeability of blood brain barrier (BBB), which increases the trafficking of lymphocytes and monocytes to the CNS. Again, opioids lower the CNS penetration of several anti-retroviral drugs to facilitate basal level of ongoing HIV replication in brain. This may be responsible for

Accepted Manuscript Posted Online

Journal of Virology

JVI

Journal of Virology

Downloaded from http://jvi.asm.org/ on March 18, 2021 by guest

1187 higher size of functional SIV reservoirs in our morphine dependent SIVmac251 infected

1188 cART treated *rhesus macaque* model.

1189

1190

1191 **Table 1: The number of brain macrophages and % of contaminating CD3+ T cells**

1192 **in the MØ-QVOA for each animal is described along with the corresponding IUPM**

1193 **values.**

1194

| Serial # | Animal_ID | % of contaminating CD3+ T cells in CD11b+ cells by TCRβ RNA level | Probability of presence of a CD4+ T cells with Intact proviral genome in Mø-QVOA | # of cells used in Mø-QVOA | IUPM for CD11b+ macrophages |
|---|---|---|---|---|---|
| 1 | CK03 | 0.071 | Less than 1 | 1.67E+07 | 0.185 |
| 2 | CK07 | 0.079 | Less than 1 | 1.00E+07 | 0.101 |
| 3 | CK40 | 0.072 | Less than 1 | 1.67E+07 | 0.144 |
| 4 | CI04 | 0.19 | Less than 1 | 1.67E+07 | 0.219 |
| 5 | CI47 | 0.118 | Less than 1 | 3.33E+07 | 0.444 |
| 6 | CK22 | 0.034 | Less than 1 | 2.33E+06 | 0.602 |
| 7 | CK31 | 0.02 | Less than 1 | 1.00E+07 | 1.194 |
| 8 | CK48 | 0.015 | Less than 1 | 3.33E+06 | 3.33 |
| 9 | CH89 | 0.019 | Less than 1 | 1.67E+07 | 1.569 |
| 10 | CI83 | 0.205 | Less than 1 | 1.67E+07 | 0.473 |
| 11 | CI90 | 0.003 | Less than 1 | 1.67E+07 | 0.227 |

1195

1196

1197

Accepted Manuscript Posted Online

Journal of Virology

JVI

Journal of Virology

1198

1199

1200

1201

Downloaded from http://jvi.asm.org/ on March 18, 2021 by guest

Accepted Manuscript Posted Online

Journal of Virology

JVI

Journal of Virology

Downloaded from http://jvi.asm.org/ on March 18, 2021 by guest

1202 **Table 2: Description of rhesus macaques used in the study**

| Serial # | Animal ID | Age (Years) | *Mamu* genotypes | | | Treatment group | Antiretroviral therapy | Peak Plasma Viral load (Copies/ml) | Plasma Viral load at necropsy (Copies/ml) | Peak CSF Viral load (Copies/ml) | CSF Viral load at necropsy (Copies/ml) |
|---|---|---|---|---|---|---|---|---|---|---|---|
| | | | *A01 | *B08 | *B17 | | | | | | |
| **1** | 12N067 | 7 | + | - | - | Saline | None | 9.02E+06 | 4.24E+04 | 1.38E+05 | 1.19E+04 |
| **2** | 15N223 | 5 | - | - | - | Saline | None | 7.22E+06 | 1.04E+05 | 1.82E+04 | 7.37E+03 |
| **3** | 14T014 | 5 | - | - | - | Saline | None | 1.89E+07 | 3.22E+08 | 6.49E+04 | 1.81E+04 |
| **4** | 14X006 | 5.2 | - | - | - | Saline | None | 3.37E+07 | 5.11E+08 | 2.45E+04 | 2.57E+05 |
| **5** | CI47 | 4.2 | - | + | - | Saline | TFV+FTC+DTG | 2.31E+07 | <LOD | 3.60E+03 | <LOD |
| **6** | CK03 | 4.3 | - | - | - | Saline | TFV+FTC+DTG | 9.87E+06 | <LOD | 1.64E+05 | <LOD |
| **7** | CI04 | 4.4 | - | - | - | Saline | TFV+FTC+DTG | 8.69E+06 | <LOD | 3.48E+05 | <LOD |
| **8** | CK07 | 4.4 | - | - | - | Saline | TFV+FTC+DTG | 1.83E+07 | <LOD | 2.03E+05 | <LOD |
| **9** | CK40 | 4.2 | - | - | - | Saline | TFV+FTC+DTG | 1.25E+07 | <LOD | 1.03E+05 | <LOD |
| **10** | 14X002 | 5 | - | - | - | Morphine | None | 8.68E+07 | 1.80E+06 | 1.13E+05 | 9.25E+04 |
| **11** | 13T005 | 5.3 | NA | NA | NA | Morphine | None | 1.85E+07 | 3.05E+06 | 4.51E+06 | 5.21E+02 |
| **12** | 14X043 | 5 | - | - | + | Morphine | None | 8.10E+05 | 3.18E+04 | 9.97E+03 | 4.12E+03 |
| **13** | 15N012 | 4.4 | - | - | - | Morphine | None | 1.02E+07 | 3.07E+05 | 1.22E+05 | 1.27E+02 |
| **14** | CK31 | 4.1 | + | - | - | Morphine | TFV+FTC+DTG | 2.00E+07 | <LOD | 7.85E+02 | <LOD |

Accepted Manuscript Posted Online

| | | | | | | | | | | | |
|---|---|---|---|---|---|---|---|---|---|---|---|
| **15** | CK22 | 4.2 | - | + | - | Morphine | TFV+FTC+DTG | 4.25E+06 | <LOD | 1.91E+03 | <LOD |
| **16** | CK48 | 4.2 | + | - | - | Morphine | TFV+FTC+DTG | 3.92E+06 | <LOD | 3.08E+05 | <LOD |
| **17** | CI83 | 4.3 | - | - | - | Morphine | TFV+FTC+DTG | 1.20E+07 | <LOD | 1.05E+04 | <LOD |
| **18** | CI90 | 4.2 | - | - | - | Morphine | TFV+FTC+DTG | 1.07E+06 | <LOD | 9.62E+03 | <LOD |
| **19** | CH89 | 4.4 | - | - | - | Morphine | TFV+FTC+DTG | 1.81E+07 | <LOD | 7.47E+04 | <LOD |

1203 All animals were male; NA: Not available; LOD: Limit of detection; TFV: Tenofovir alafenamide; FTC: Emtricitabin; DTG: Dolutegravir.



Downloaded from http://jvi.asm.org/ on March 18, 2021 by guest

Journal of Virology JVI Journal of Virology

Accepted Manuscript Posted Online

Journal of Virology

JVI

Journal of Virology

Downloaded from http://jvi.asm.org/ on March 18, 2021 by guest

1204 **Table 3: The details of all fluorochrome-conjugated monoclonal antibodies used**

1205 **in the flow cytometry experiments.**

| Antibody | Fluorophore | Clone | Vendor | Catalog # |
|---|---|---|---|---|
| CD45 | BV786 | D058-1283 | BD Horizon | 563861 |
| CD3 | AF700 | SP34-2 | BD Pharmingen | 561805 |
| CD3 | APC-Cy7 | SP34-2 | BD Pharmingen | 557757 |
| CD4 | PE-CF594 | L200 | BD Biosciences | 562402 |
| CD4 | AF700 | L200 | BD Pharmingen | 560836 |
| CD8 | BV510 | SK1 | BD Horizon | 563919 |
| CD20 | BUV805 | 2H7 | BD Horizon | 612905 |
| CD25 | BV421 | BC96 | Biolegend | 302612 |
| NKG2a (CD159a) | PC7 | Z1999 | Beckman coulter | B10246 |
| CD127 | PC5 | R34.34 | Beckman coulter | A64617 |
| CD38 | APC | OKT10 | NHP Reagent resource | Not available |
| CD95 | FITC | DX2 | BD Pharmingen | 556640 |
| HLA-DR | PE-Texas Red | TU36 | Life Technologies | MHLDR17 |
| IFNγ | PE | B27 | BD Pharmingen | 562016 |
| IL-4 | FITC | MP4-25D2 | BD Biosciences | 554484 |
| IL-17 | APC | eBio64Dec17 | Invitrogen | 17-7179-42 |
| TNF-α | FITC | Mab11 | BD Pharmingen | 554512 |
| FOXP3 | APC | PCH101 | eBioscience | 17-4776-42 |
| CXCR5 | PE | 710D82.1 | NHP Reagent resource | Not available |
| CXCR5 | BV421 | J25D4 | Biolegend | 356919 |
| PD-1 | PerCP/Cy5.5 | EH12.2H7 | Biolegend | 329913 |
| CTLA-4 | PE-Cy5.5 | BNI3 | Biolegend | 369607 |
| CXCR3 | BUV 393 | 1C6 | BD Biosciences | 565223 |
| CCR4 | PE | 1G1 | BD Biosciences | 561110 |
| CCR6 | PE-Cy7 | 11A9 | BD Pharmingen | 560620 |

1206

Accepted Manuscript Posted Online

Journal of Virology

JVI

Journal of Virology

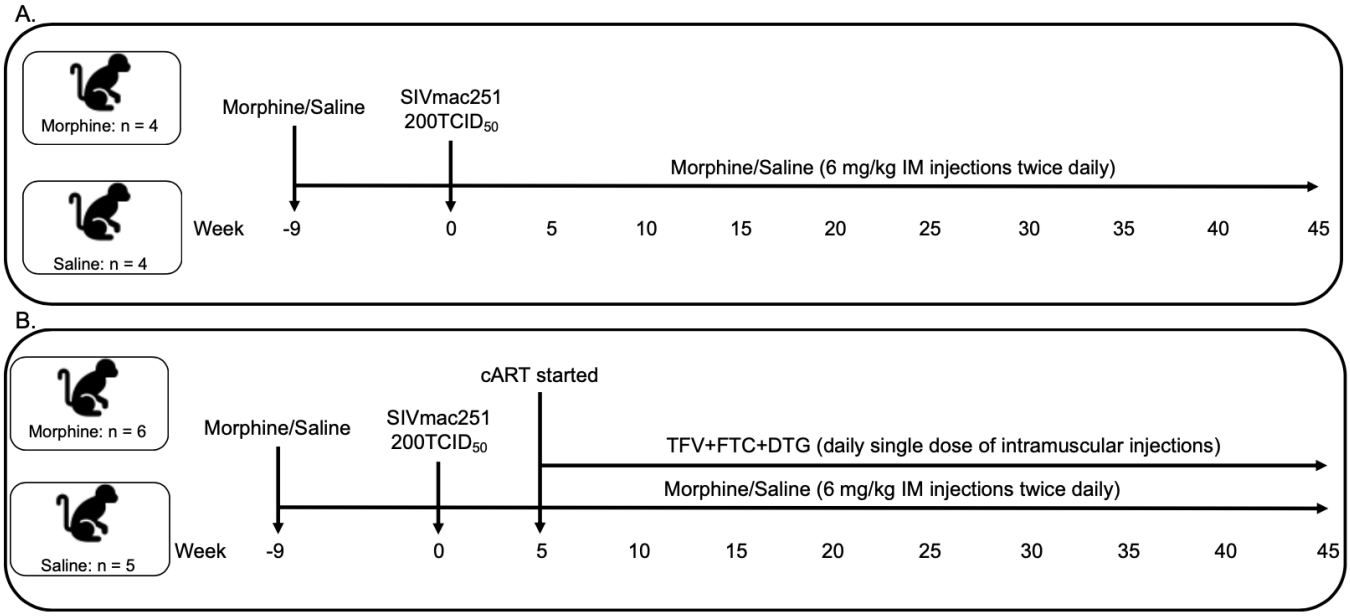


Downloaded from http://jvi.asm.org/ on March 18, 2021 by guest

Accepted Manuscript Posted Online

Journal of Virology

JVI

Journal of Virology

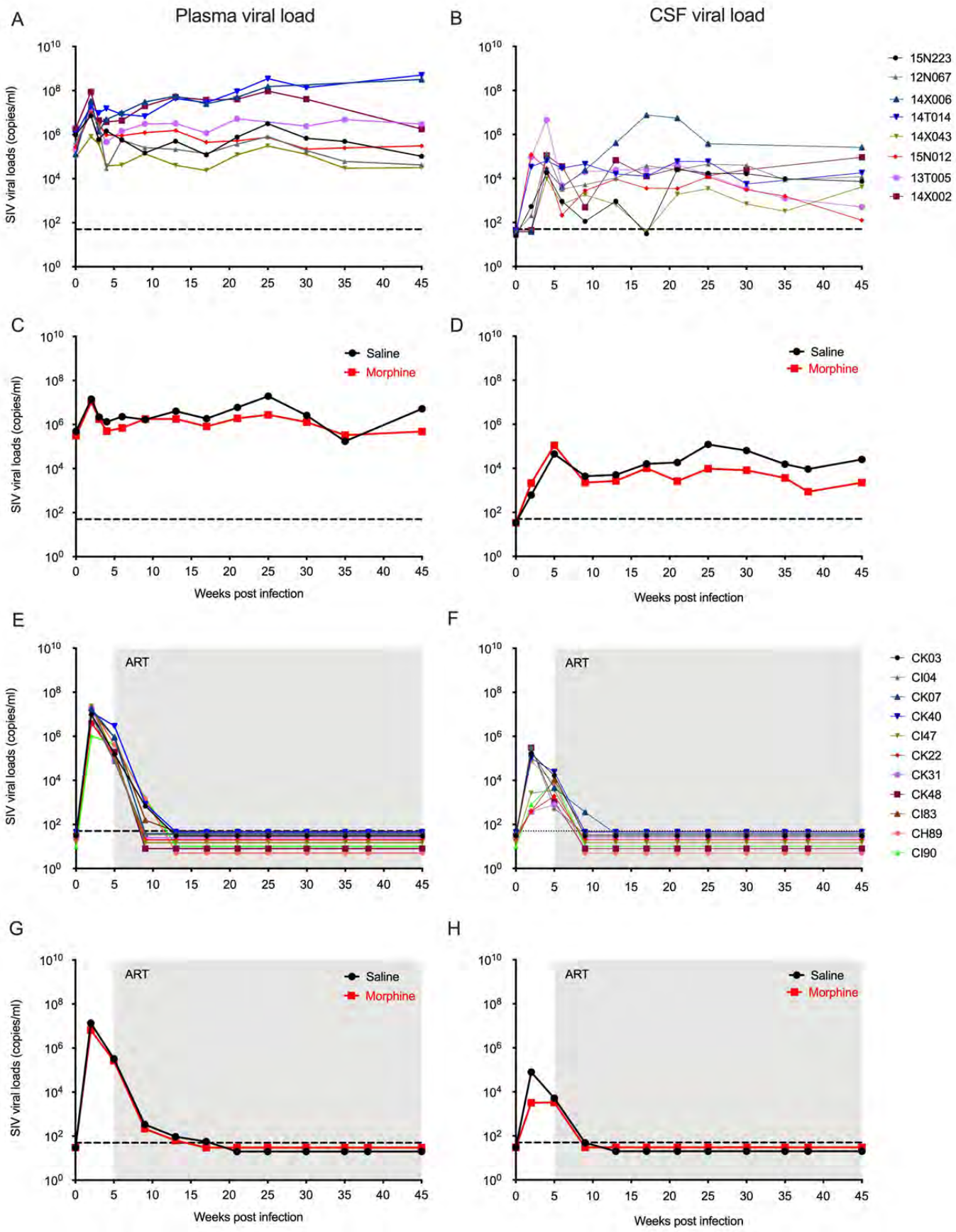


Downloaded from http://jvi.asm.org/ on March 18, 2021 by guest

Accepted Manuscript Posted Online

Journal of Virology

JVI

Journal of Virology

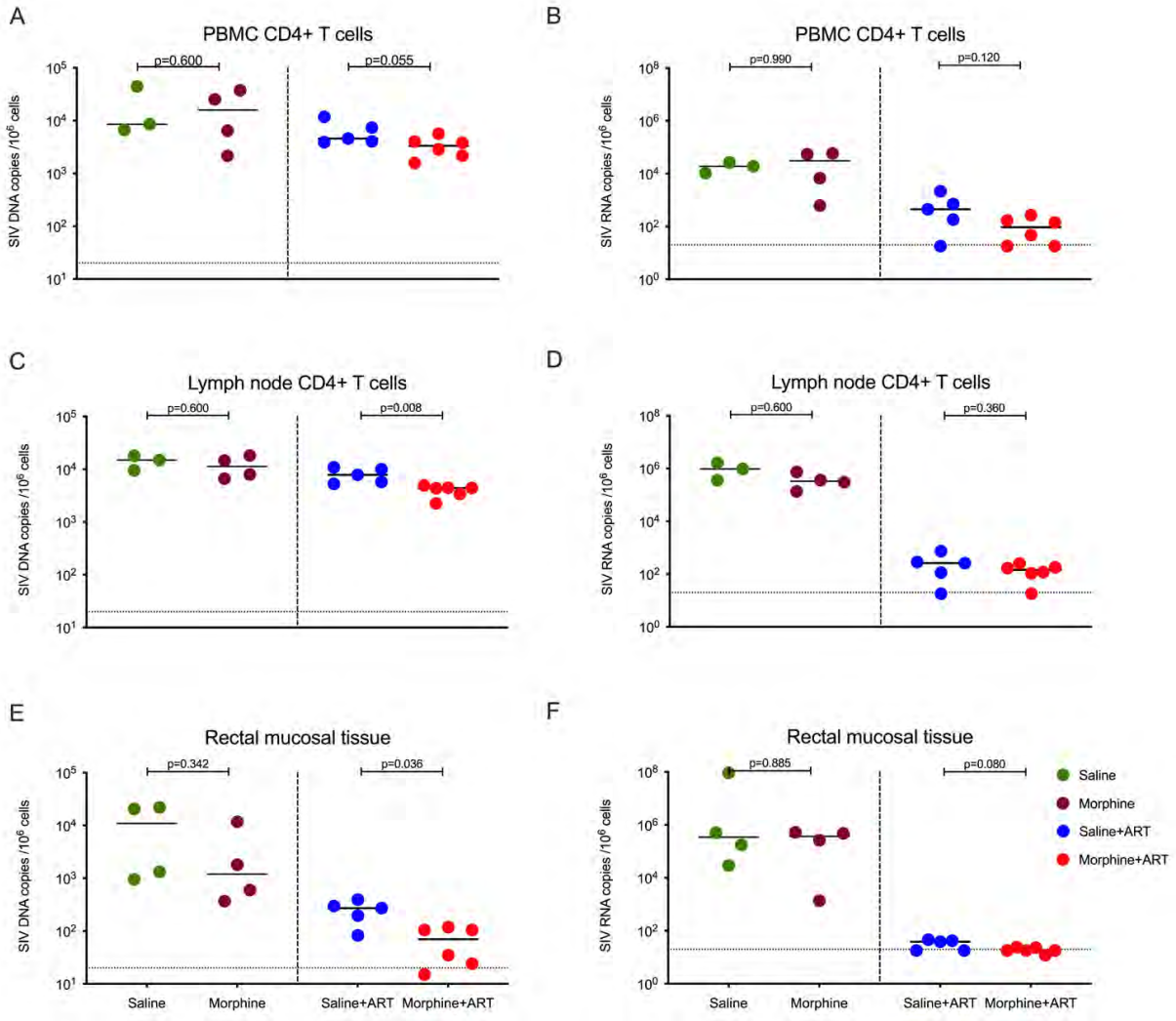


Downloaded from http://jvi.asm.org/ on March 18, 2021 by guest

Accepted Manuscript Posted Online

Journal of Virology

JVI

Journal of Virology

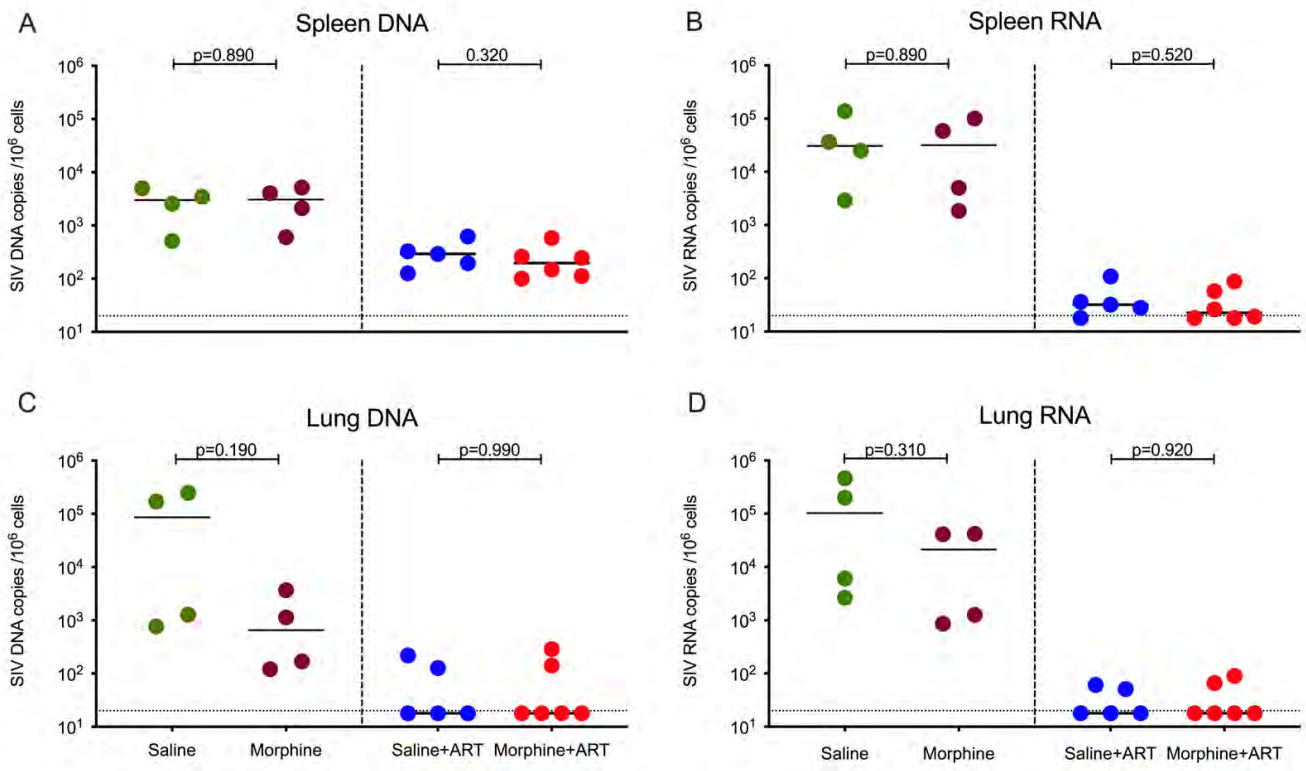


Downloaded from http://jvi.asm.org/ on March 18, 2021 by guest

Accepted Manuscript Posted Online

Journal of Virology

JVI

Journal of Virology

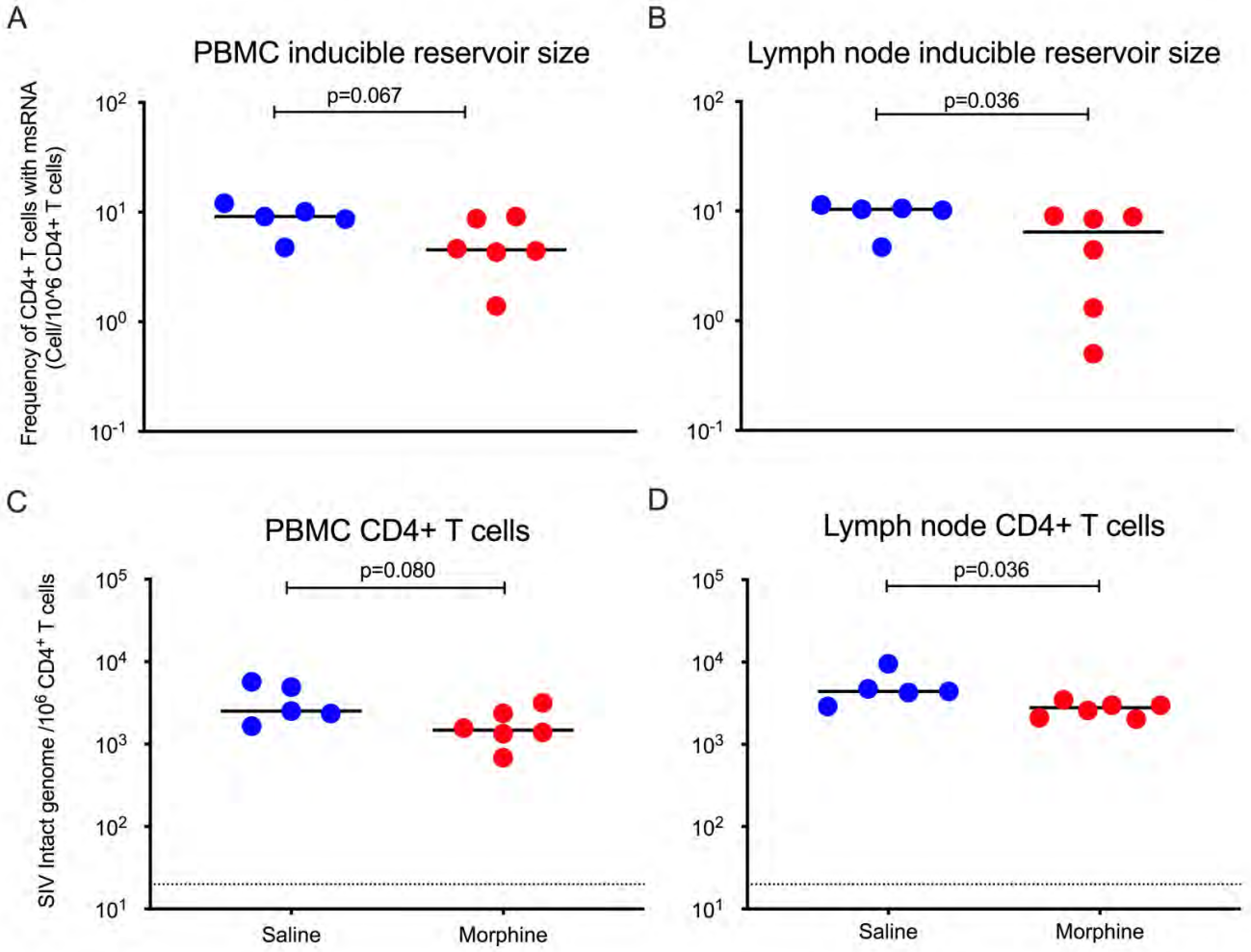


Downloaded from http://jvi.asm.org/ on March 18, 2021 by guest

Accepted Manuscript Posted Online

Journal of Virology

JVI

Journal of Virology

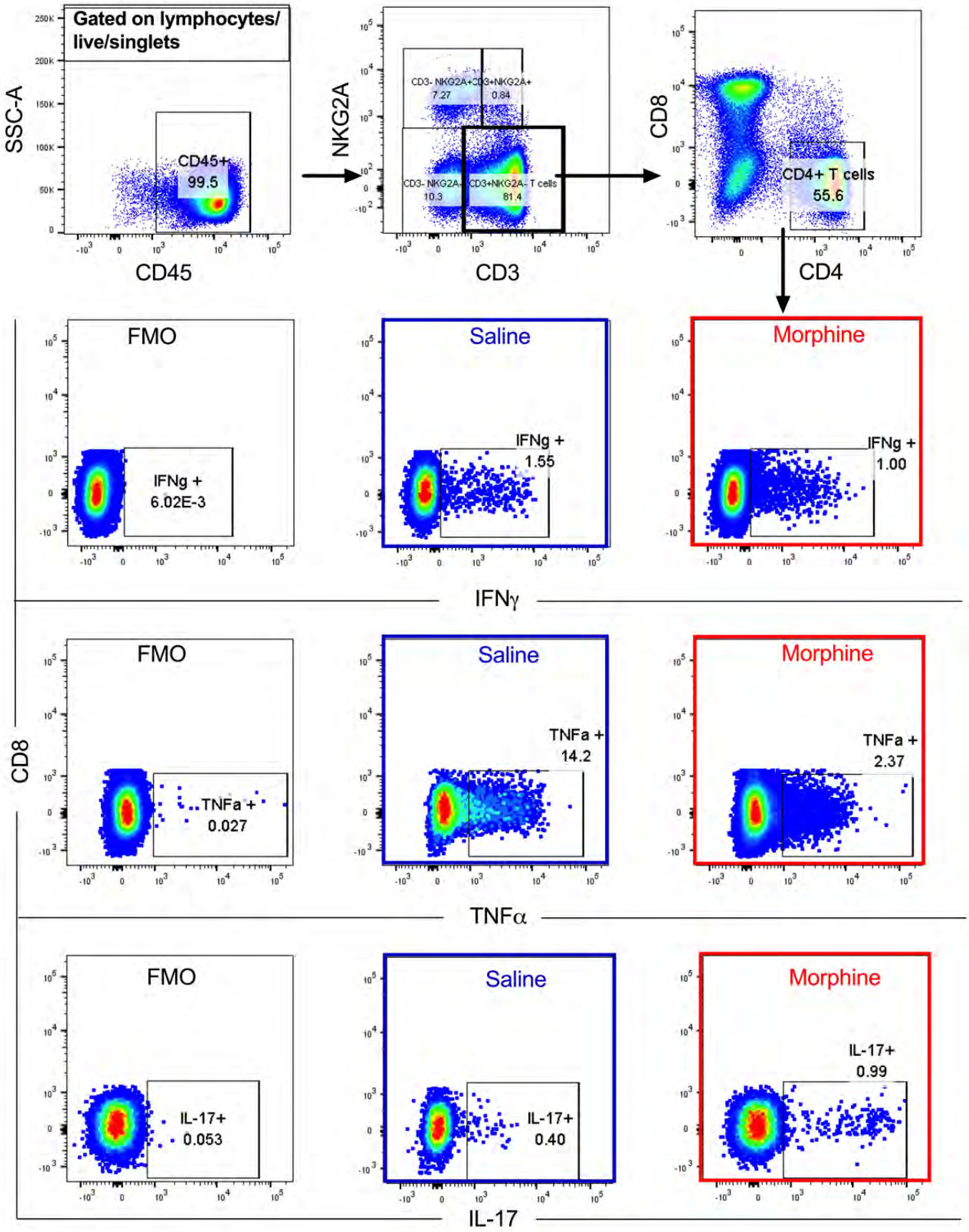


Downloaded from http://jvi.asm.org/ on March 18, 2021 by guest

Accepted Manuscript Posted Online

Journal of Virology

JVI

Journal of Virology

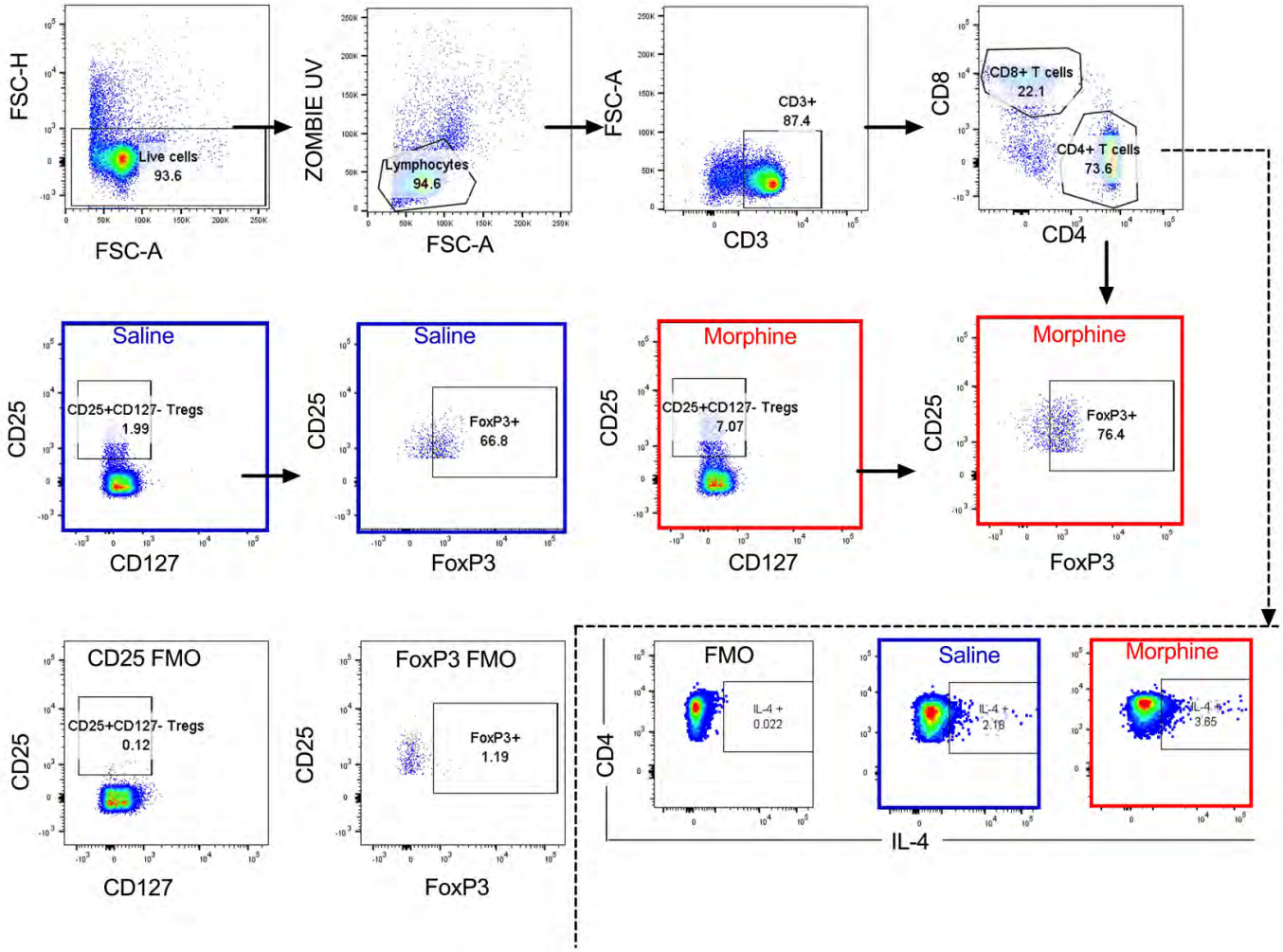


Downloaded from http://jvi.asm.org/ on March 18, 2021 by guest

Accepted Manuscript Posted Online

Journal of Virology

JVI

Journal of Virology

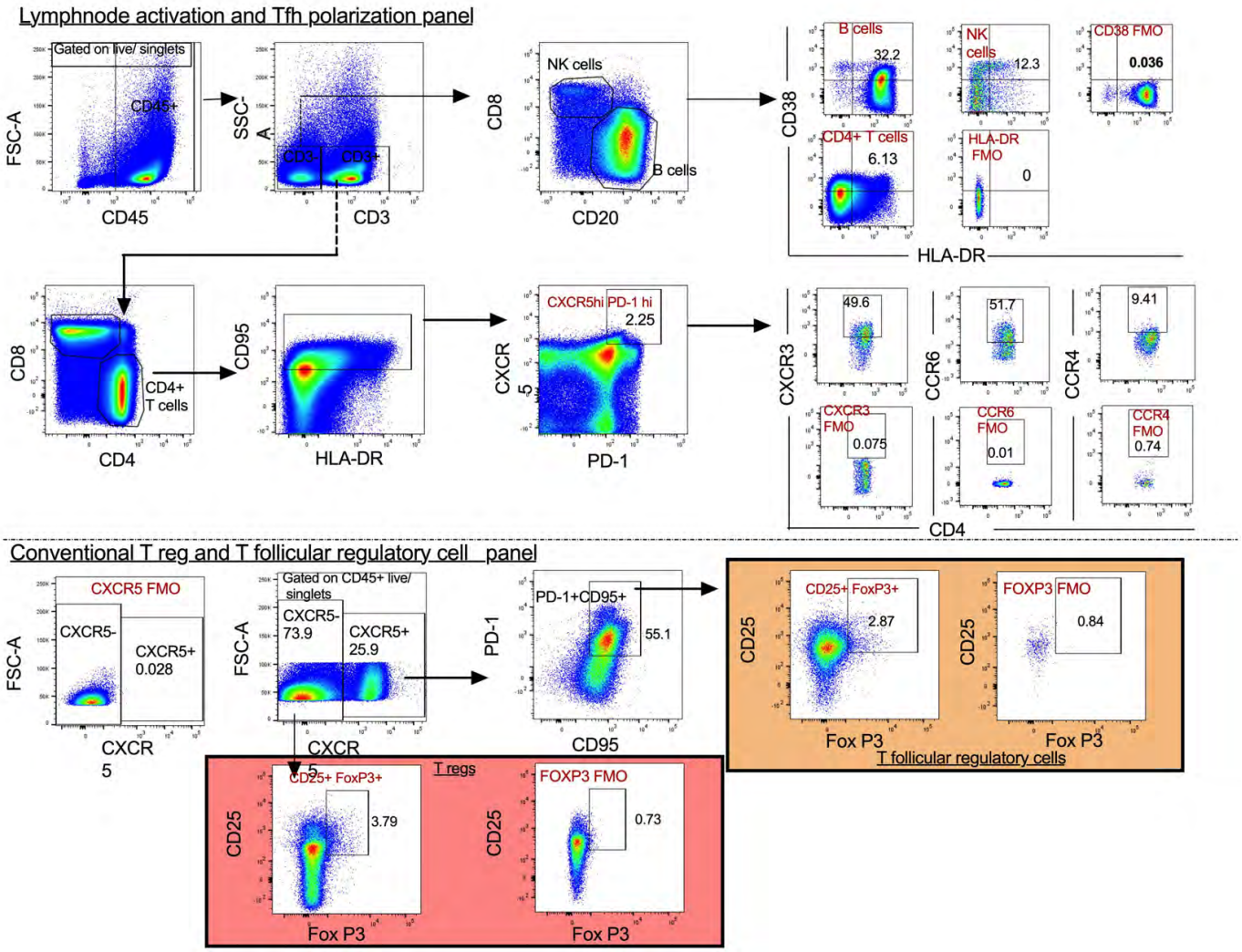


Downloaded from http://jvi.asm.org/ on March 18, 2021 by guest

Accepted Manuscript Posted Online

Journal of Virology

JVI

Journal of Virology

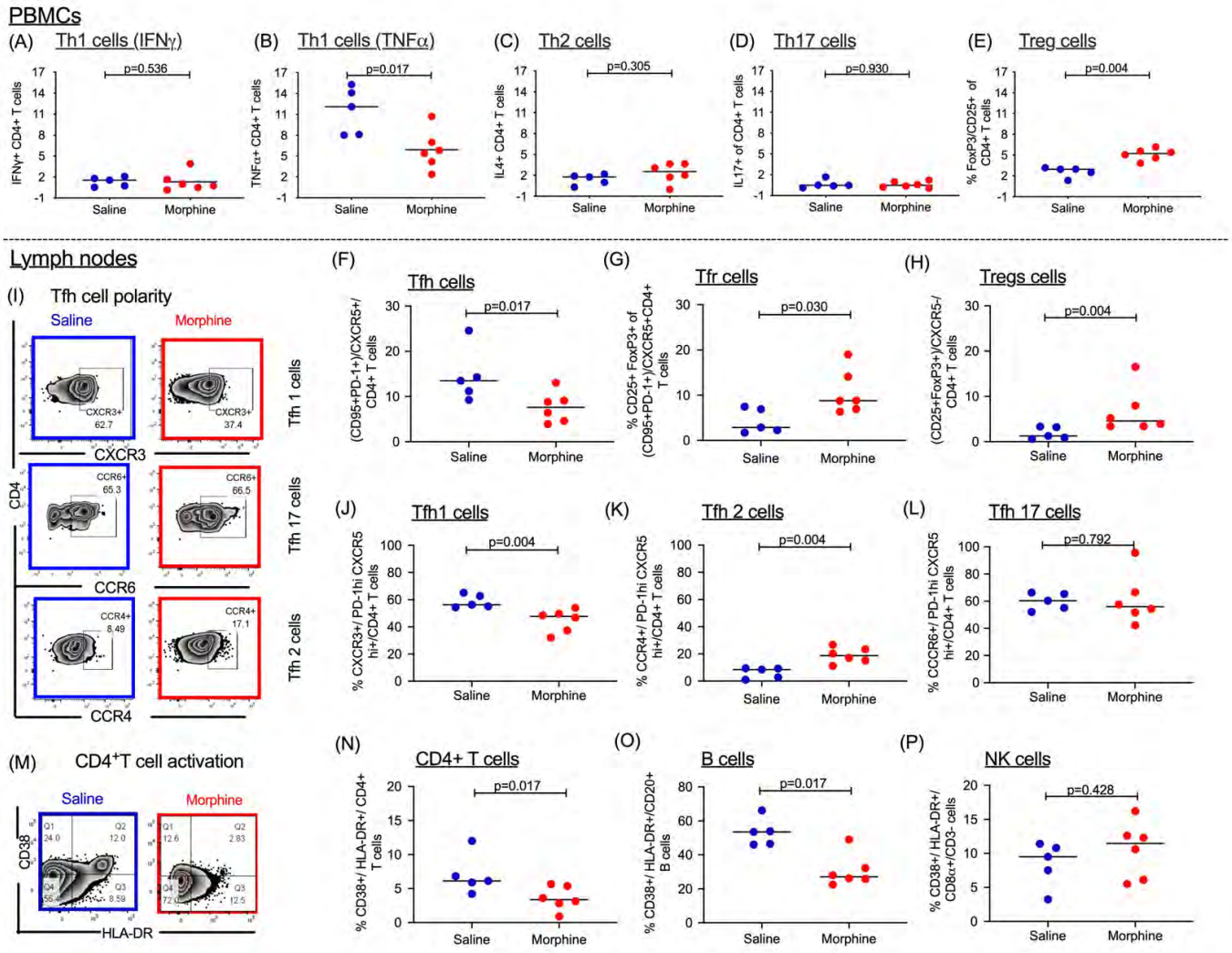


Downloaded from http://jvi.asm.org/ on March 18, 2021 by guest

Accepted Manuscript Posted Online

Journal of Virology

JVI

Journal of Virology

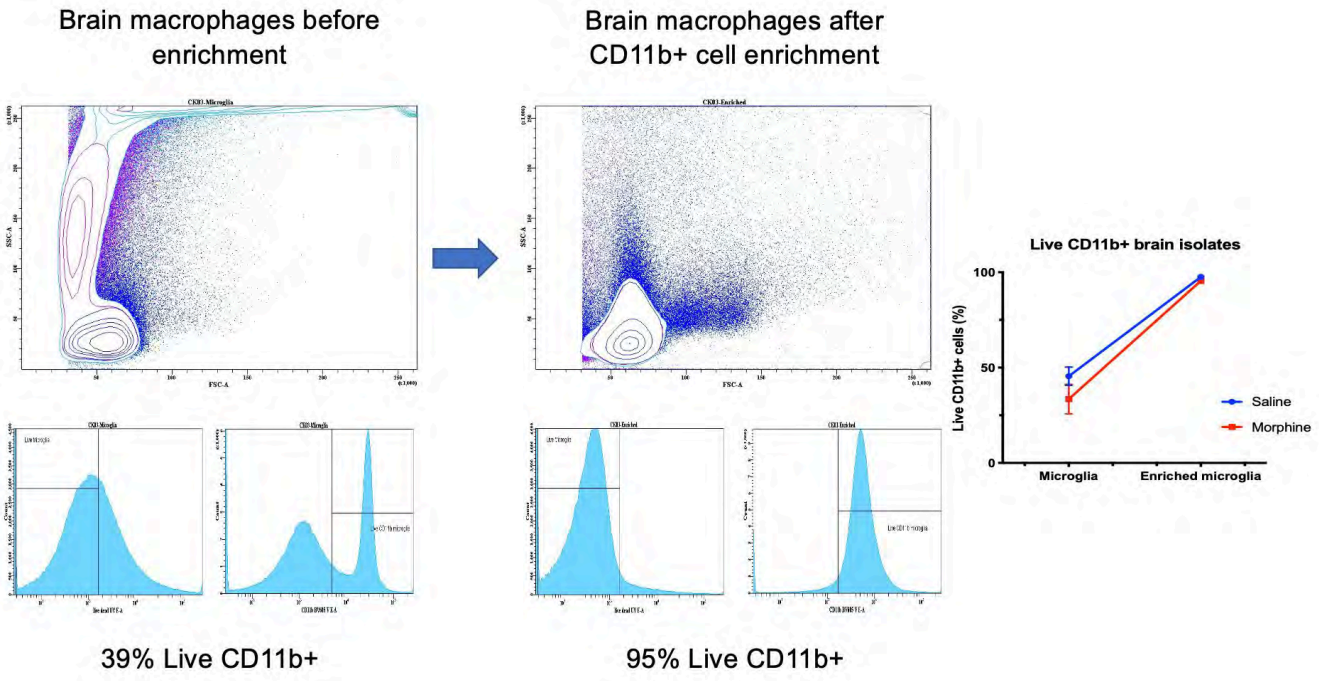


Downloaded from http://jvi.asm.org/ on March 18, 2021 by guest

Accepted Manuscript Posted Online

Journal of Virology

JVI

Journal of Virology

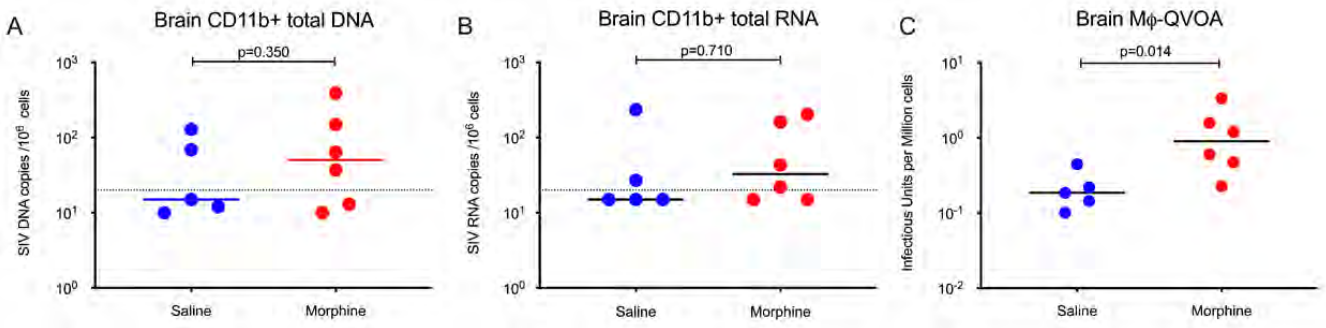


Downloaded from http://jvi.asm.org/ on March 18, 2021 by guest

Accepted Manuscript Posted Online

Journal of Virology

JVI

Journal of Virology

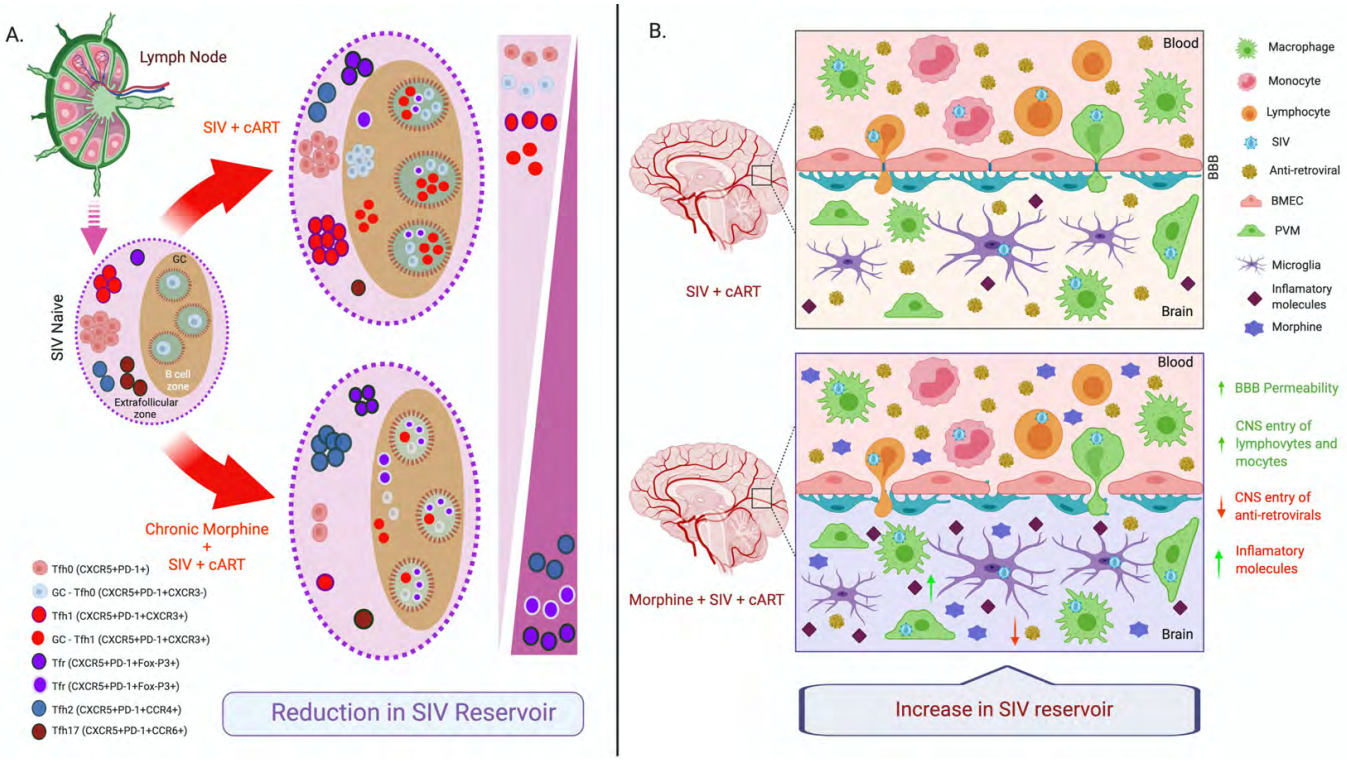


Downloaded from http://jvi.asm.org/ on March 18, 2021 by guest